Large-scale implementation of mechanized micro-rainwater harvesting structures for improving soil health by enhancing carbon sequestration in the Jordan Badia

Davie Vuurboom

Universiteit Utrecht

ICARDA
Science for resilient livelihoods in dry areas

Large-scale implementation of mechanized micro-rainwater harvesting structures for improving soil health by enhancing carbon sequestration in the Jordan Badia

MSc Thesis
July – 2022

Author: Davie Vuurboom
Student number: 5719585
E-mail: d.j.vuurboom@students.uu.nl

First supervisors: Geert Sterk & Rens van Beek
Second supervisor: Mira Haddad

MSc Programme: Earth Surface and Water

Faculty of Geosciences
Department of Physical Geography
Utrecht University

Preface

Here I present my Master's thesis, an important part of the Master's programme Earth Surface and Water at Utrecht University. The first part of this trajectory started excitedly with a 10 week trip to Amman, Jordan where I conducted field measurements and was able to enjoy the beautiful landscapes of Jordan and the hospitality of the Jordanian people. I made new friends, and was able to meet and learn a lot from my two local supervisors from ICARDA: Mira Haddad and Stefan Strohmeijer (who I would like to thank here!).

On my return, the research continued and on a daily basis I could ask all of my questions to Geert Sterk, my first supervisor. However, not long after, the terrible news reached us that Geert was terminally ill and had stopped working. After a short sickbed Geert died on May 2nd 2022.

Thank you Geert for the opportunities you created for me and the other students.

After Geert the research continued under the guidance of Rens van Beek. I was lucky enough to receive lots of thoughtful feedback which helped me tremendously. Thank you for that Rens. This resulted in the thesis before you.

I hope you find it both interesting and useful,

Davie Vuurboom
July 2022

Abstract

90% of Jordan is covered in a semi-desert area called the Badia, an Arabic word describing the land where Bedouins live. Many Bedouin families still live semi-nomadic lifestyles and practice seasonal grazing with sheep and goats. Although only 6.5% of the Jordanian population lives in the Badia, it hosts over 85% of the country's livestock. Due to changing climatic conditions and overexploitation of natural resources by humans, land degradation has decreased the palatable dry biomass production of the Jordan Badia by half from the 1990s to 2010. However, with appropriate management strategies, the Badia can be rehabilitated. One such strategy is the implementation of mechanised Micro Water Harvesting (MWH). By accumulating and storing rainwater and planting vegetation in the Badia, atmospheric carbon can be captured in the soil, carbon sequestration. Carbon sequestration is a promising method to reduce atmospheric carbon concentrations. By storing carbon in the soil, soil health, water availability, and fodder for livestock improve as well.

This study aimed to refine the method of Hall (2021). The new method is able to, with freely available data, quantify the potential amount of carbon sequestration *location specific* when MWH is implemented on a large scale. The following procedures were executed to meet the aim: (1) with a GIS-based approach and ISRIC data sets performed a land suitability evaluation based on FAO classifications, (2) the density of potential MWH structures was mapped based on the CHIRPS rainfall dataset and the Curve Number method and (3) field data was combined with climate data for the modelling of carbon stocks using the RothC-26.3 model. Combining these three procedures resulted in the potential sequestration of 0.48 Mt and 1.1 Mt of carbon in 20 years by using MWH on a large scale in the Badia. Between 9.5 and 16.5% of the Badia is suitable for structures with a spacing between 4-25 meters. The results demonstrate where and how much carbon potentially can be sequestrated, which is essential information for decision-makers. Improvements can still be made in the method for more accurate sequestration values.

Table of contents

Acronyms

CHIRPS Climate Hazards Group InfraRed Precipitation with Station

CN Curve number

ICARDA The International Centre for Agricultural Research in the Dry Areas

ISRIC **i**nternational Soil Reference and Information Centre

MENA The Middle East and North Africa

MWH mechanized micro water harvesting

RothC-26.3 Rothamsted Carbon 26.3

SOC soil organ carbon

SOM soil organic matter

TOC Total organic carbon

WH harvesting structures

1. Introduction

1.1 Background

Drylands are areas of land which receive a relatively low amount of precipitation. These arid regions cover about 45% of the Earth's land surface (Schimel, 2010) and are home to more than 38% of the global population, 90% of whom live in developing countries (Reynolds, 2007). They occur on every continent and span a diversity of cultures and landscapes. Drylands are defined by the aridity index (AI). The aridity index measures the ratio between average annual precipitation and total potential evapotranspiration. Land areas with an AI lower than 0.65 are *arid regions*. Drylands are subdivided into four categories (figure 1): hyper-arid deserts (<0.05), arid (0.05-0.20), semi-arid (0.20-0.50) and dry sub-humid (0.50-0.65) (FAO from UNEP-WCMC, 2007). Drylands primarily have three economic functions: rangelands (65% of the global drylands including deserts), farmland (both rainfed and irrigated) (25%), and sites for towns and cities (10%); this last category is growing rapidly (UN, 2011).

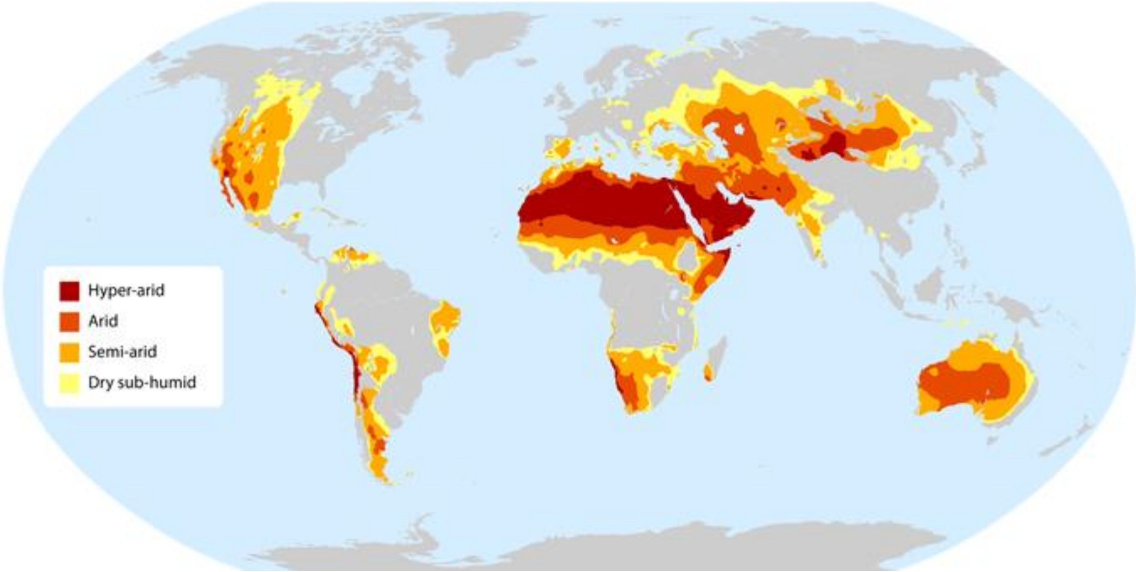

Figure 1 The world's drylands and subtypes. hyper-arid deserts (<0.05), arid (0.05-0.20), semi-arid (0.20-0.50) and dry sub-humid (0.50-0.65). Source: FAO from UNEP-WCMC (2007)

The Middle East and North Africa (MENA) region is the most water-scarce region globally. In this region, 6.3% of the world population has access to only 1.4% of the renewable freshwater resources (Roudi-Fahimi, 2002).

The dryland areas in the MENA region are vulnerable to land degradation due to water scarcity. Water scarcity also leads to sparse vegetation, withholding the soil from organic matter input and resulting in poor soil development. Poor soils have low infiltration capacity and soil aggregate stability and are prone to wind and water erosion and continued deterioration of the soil quality or health.
Many of these drylands are used for livestock grazing by local populations, and large areas have become degraded, so there is an urgent need to rehabilitate the degraded land using sustainable land management to secure the livelihood of the growing population (Zdruli, 2014; Droogers et al., 2012).

Jordan is an example of such a water-scarce country in the MENA region. More than 90% of the country is covered by the so-called Badia, an Arabic word identifying the land where Bedouins live. Many Bedouin families still live semi-nomadic lifestyles and practice seasonal grazing with sheep and goats. Although only 6.5% of the Jordanian population lives in Badia, it hosts over 85% of the country's livestock.

With the rising challenge of higher food demands in combination with water scarcity and its negative effects on the soil, the Jordanian Badia requires new management strategies. One strategy is to combat the land degradation and rehabilitate the Badia with water harvesting structures (WH). WH is the accumulation and storage of rainwater. It has been used to collect surface water or increase the replenishment of groundwater reservoirs to provide drinking water for humans and livestock, sustain irrigation, and increase the soil moisture to cultivate crops and sustain plant growth for food or fodder. (Oweis et al., 2017).

1.2 Problem description

1.2.1 Carbon sequestration as a solution

Due to rising carbon dioxide emissions and it's well documented detrimental effect on water availebillity but also by, depletion of soil nutrients, premature- and over-grazing, and overexploitation of natural resources by humans, land degradation has decreased the palatable dry biomass production of the Jordan Badia by half from the 1990s to 2010. (Shawahneh et al., 2011; Myint and Westerberg, 2014).

Carbon sequestration is a method to reduce atmospheric carbon by storing carbon in the soil. Both soil degradation and high atmospheric carbon concentration can be combatted by a method such as mechanized micro water harvesting (MWH).

A study carried out by Hall (2021) performed a remote sensing study for areas that were found suitable for MWH. The study also calculated roughly the potential carbon sequestration in the Jordan Badia using the RothC-26.3 model. The results indicated that 51.20% of the country is suitable for implementing MWH structures (figure 3). This would lead to a 0.65 t/ha increase of carbon storage in the soil increasing the storage potential by 2,973,100 tons.

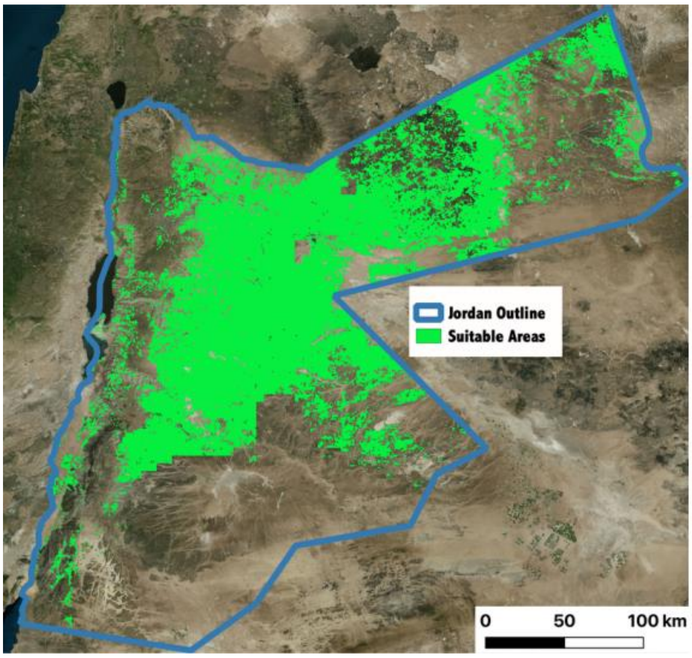

Figure 2 Suitable area for MWH from the study of Hall (2021)

Although these are promising results, these calculations assume that all soils in the Badia are homogenous. However, not all areas are equally suitable for MWH because some areas lack sufficient rainfall or soils are too pervious for storing moisture. This results in areas with different successes of vegetation and thus sequestration values. Hence, the potential carbon sequestration as calculated by Hall (2021) may be overestimated. Soil quality is not only specified by the physical and chemical properties of the soil but also is heavily influenced by the composition of clay minerals and organic matter content.

With this knowledge and available soil and climatical data, an MWH suitability classification of the Jordanian Badia is needed to conduct a more accurate potential carbon sequestration assessment and locate the areas where the most significant impact can be made.

1.3 Objectives

This study aims to refine the work of Hall (2021) by developing a method that can quantify the potential amount of carbon sequestration specific to any particular *location* when MWH is implemented. In this thesis, the Jordan Badia is used as case study. To achieve this aim, the following objectives are set:

I) Classify the Jordan Badia into different suitability categories for MWH (and thus carbon sequestration) based on physical soil and climatical characteristics.
II) Determine optimal dimensions of the Vallerani MWH structures for successful plant growth based on the rainfall-runoff ratio.
III) Quantify potential location-specific carbon sequestration for the Jordan Badia.

1.4 Mechanized Micro Water Harvesting

MWH is the accumulation and storage of rainwater. It has been used to collect surface water or increase the replenishment of groundwater reservoirs to provide drinking water for humans and livestock, sustain irrigation, or increase the soil moisture, which due to better soil health, in turn, can increase crop and fodder production allowing for more livestock (Oweis et al., 2017).

The International Centre for Agricultural Research in the Dry Areas (ICARDA) is researching the effects of mechanised Micro Water Harvesting (MWH), also known as the Vallerani system. This is a cost-effective and efficient solution to land degradation. It has shown promising results in previous studies (Sprong, 2019; Hall, 2021; Strohmeier et al., 2021). The Vallerani implementation uses a modified plough pulled by a heavy-duty tractor. The tractor follows the contour lines, and the plough creates a furrow about 20-30 cm deep (Figure 3A) and 4.5 m long. The excavated material accumulates on the downhill side, forming a ridge that stops and collects runoff (Figure 3B). When a furrow (pit) overflows from abundant rainfall, the water flows into the next furrow. Shrub seedlings are planted in pits along the ridges. With the moisture available, they can grow rapidly, helping to conserve soil and provide food for livestock.

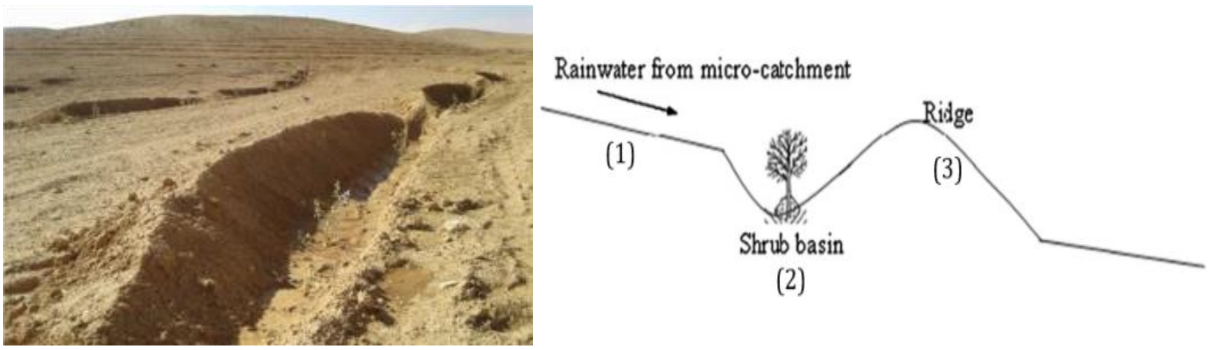

Figure 3A Fresh Vallerani mechanized micro water harvesting furrow, Source ICARDA (left) and 2B (right) schematic overview of a micro rainwater harvesting structure. (Taken from Ali et al., 2010)

Previous research on the effect of MWH on soil water dynamics (Sprong, 2019; Strohmeier et al., 2021) shows that the water harvesting structures positively influence water availability in the soils by almost halving the period of water stress. This extra availability sustains higher daily evapotranspiration rates and reduces heat stress for the vegetation. The vegetation benefits the most from the extra moisture stored in the pits (shrub basin). Strohmeier et al. (2021) documented an expansion of vegetation in the upslope direction. New recruitment and the emergence of vegetation upslope may further enhance the soil moisture, at least during rainfall periods, through rainfall interception, surface runoff deceleration and local infiltration.

1.5 Carbon sequestration

Several studies (Faloon et al., 2007; Cornelis et al., 2013) have proposed that these structures can also have the additional benefit of promoting soil carbon sequestration. Soil carbon sequestration (C-sequestration) is the process of turning atmospheric carbon dioxide (CO_2) into soil organic matter (SOM) through photosynthesis (Jastrow et al., 2007), see Figure 4. It is well established that SOM is a crucial component of healthy soil, which is essential as it increases agricultural production and improves water quality (Ontl and Schulte, 2012). When vegetation biomass increases, it extracts CO_2 from the atmosphere. Plants fix organic carbon in soils through debris roots and fluids, and soil fauna decays these residues into soil organic matter. Some of this SOM remains as soil organ carbon (SOC), and another part is released into the atmosphere as CO_2. The potential of CO_2 storage in soils is well documented, but sequestration amounts differ significantly by soil and land use type (Sleutel et al., 2003; Wiesmeier et al., 2014; Kelland et al., 2020).

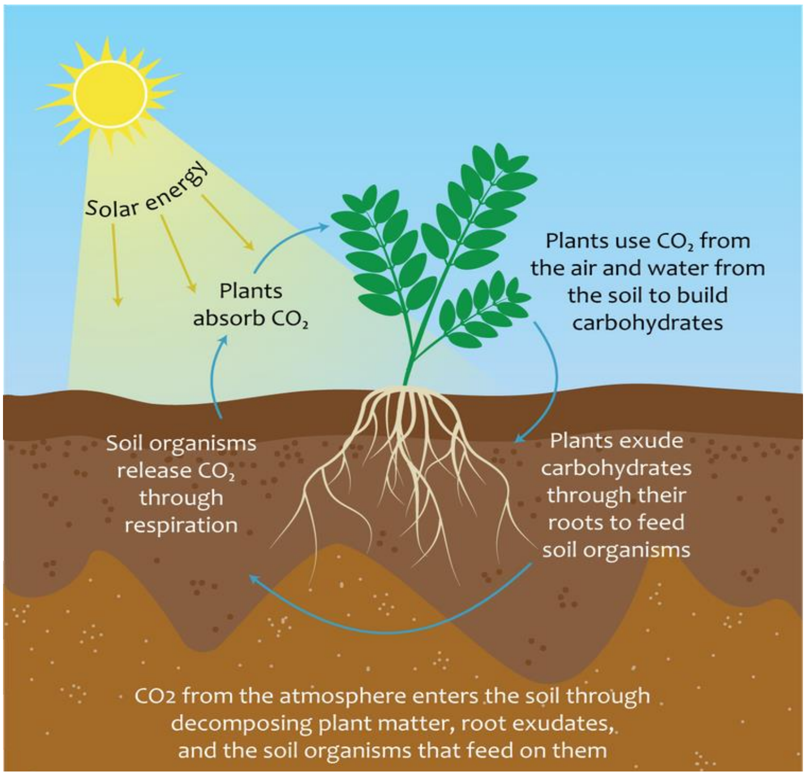

Figure 4 Soil carbon sequestration (Lavallee, 2020)

Soils contain approximately 2344 Gt SOC globally (Stockmann et al., 2013). Small changes in the soil organic carbon stock could result in significant impacts on the atmospheric carbon concentration. Soils have a large storage capacity, and enhancing soil storage by even a few percentage points could make a big impact. Over the last 10,000 years, agriculture and land management strategies have decreased SOC by 840 Gt globally. The historic loss of a SOC pool for the soils of the MENA region may be 6-12 Gt compared with the global loss of 66-90 Gt. assuming that 60 percent of the historic loss can be re-sequestrated, the total soil carbon sink capacity of the MENA region may be 3-7 Gt. Estimated is potential carbon sequestration in the MENA region 0.2-0.4 Gt carbon per year (Lal, 2002).

2. Study area

2.1 Jordan

This study was done on two levels. The first level is based on GIS analyses and was focused on the Jordan Badia, while the second level of research was based on fieldwork activities at the research site.

Jordan, or formally the Hashemite Kingdom of Jordan, is a landlocked country that lies 80 km east of the Mediterranean Sea, between 29º 10'N – 33º 45'N and 34º 55'E – 39º 20'E (Figure 5). It has an area of 89.329 km^2 and a population of 11.2 million (Al-Homoud et al., 1995; Statistics Do. Statistical Yearbook of Jordan, 2022). Jordan is divided into two areas: the Badia and the non-Badia. This research is focused on the Jordan Badia, which comprises around 90% of the country's area. The Badia itself is subdivided into three regions: the Northern Badia, which comprises 35.7% of the area (25,930 km^2), the Middle Badia, which comprises 13.3% (9,634 km^2), and the Southern Badia, which comprises 51.0% (37,096 km^2). Jordan's climate ranges from a Mediterranean to a desert climate; the Badia region is, with a maximum of 200 mm rainfall annually, arid. Jordan has a unique topography. The Western part of the country has the world's lowest valley, with an elevation down to 400m below sea level. To the East of the Jordan valley, mountain ranges reach up to 1500 metres above sea level. To the East of this mountain range is a semi-desert plateau that covers approximately 80% of the country (Freian and Kadioglu, 2008). Yearly air temperatures fluctuate widely from a minimum average of 10°C to 24.5°C, showing a strong inter-annual variability. Precipitation rates decrease from North to South, West to East, and higher to lower altitudes. Annual rainfall ranges from 250 to 450 millimetres in the North-Western area and reduces to below 100 millimetres in the East. In the South, precipitation can be as low as 50 mm annually.

Figure 5 Aerial map composite of Jordan and Al Majidiyya research area. Source: Bingmap with the research site highlighted

Figure 6 shows the land cover of Jordan. The Badia's surface mainly consists of chert plain, bare soil and basaltic plain. In the Jordan valley, there are some rainfed and irrigated agricultural lands. Next to the Jordan valley, in the North the so-called build-up areas are located as well.

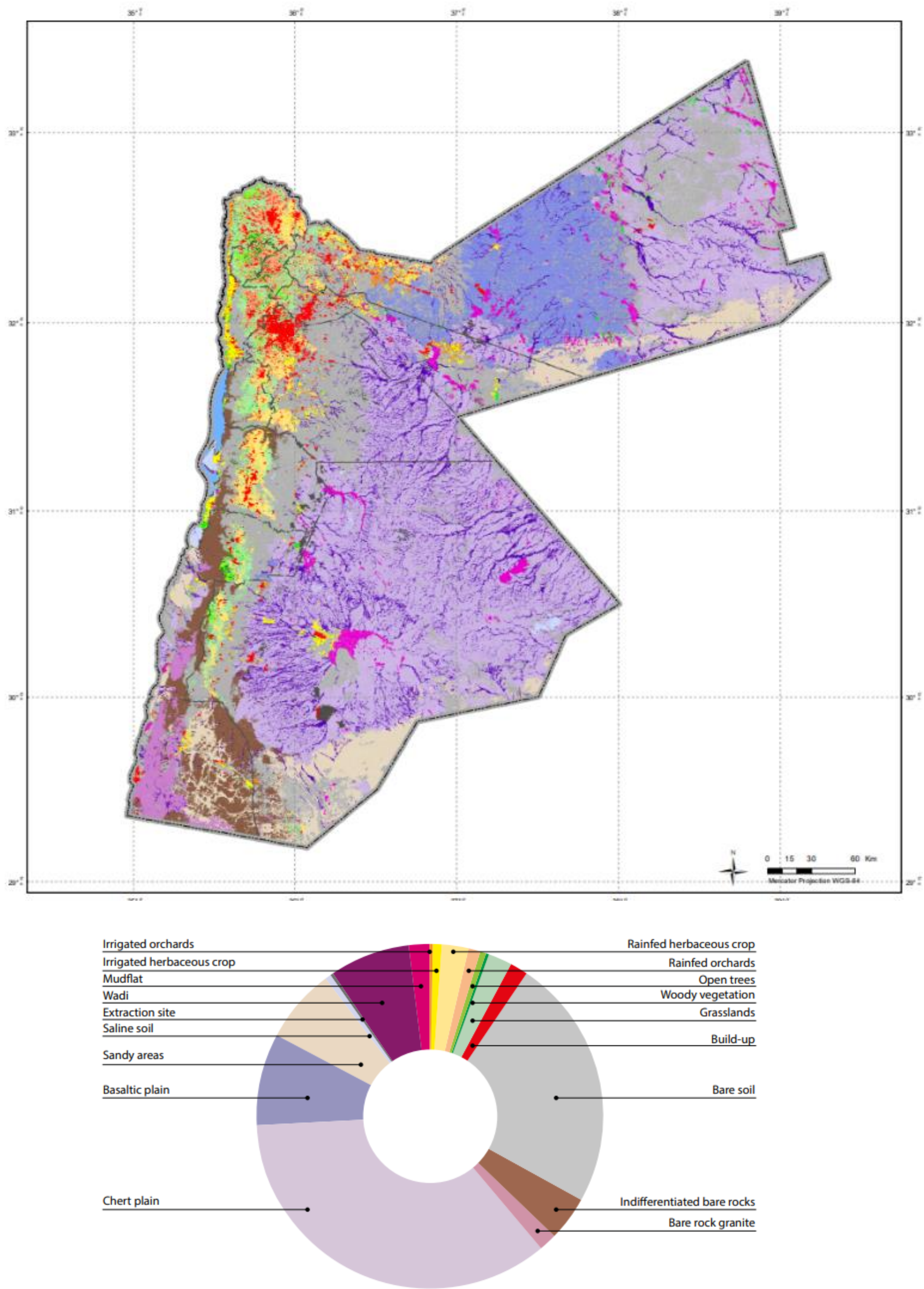

Figure 6 Land cover map by Franceschini (2019), FAO Land cover Atlas

2.2 Research site

In November 2016 a 28.6 ha large catchment (31°43'3.48"N / 36° 7'35.75"E) was treated using the 'Vallerani Delfino-Plow' system (Antinori and Vallerani, 1994) for mechanized Micro Water Harvesting (MWH) implementation. This field is called Al Majidiyya (Figure 5) and is located approximately 30 km to the South-East of Amman. The climate is arid (UNEP, 1992), with the average annual rainfall between 1999 and 2018 being 142.8 mm (Strohmeier et al., 2021). Most precipitation falls between December and February (Karrou et al., 2011). Over the past thirty years, the average daily minimum and maximum temperatures are 8.5°C and 25°C (Haddad, 2019). The local altitude is approximately 850 m above sea level, and the average slope is 4°, indicating an area consisting of gentle slopes. Hilltops are eroded and rocky, while more downstream soils have deeper depths (exceeding 2.0 m). Soil type is a calcisol with a silt loam, silty clay loam, or clay loam texture (IUSS Working Group WRB, 2015) which is a widespread type in the MENA region (Zdruli, 2014). The land cover comprises rangelands with the sporadic presence of barley crops cultivated by local farmers for livestock fodder. Spontaneous vegetation cover is small and sparse, mainly consisting of small grass patches appearing during the rainy seasons in a few locations. Al Majidiyya was appointed by ICARDA as a research area for the effect of Vallerani structures on rangeland rehabilitation and is planted with native shrub seedlings, such as saltbush A. halimus.

A. halimus plants are distributed widely in temperate and subtropical saline habitats (Mulas and Mulas, 2004). A. halimus is characterised by high biomass production and high tolerance to drought and saline soils. (de Romero, 1981). The shrubs can provide a high quantity of biomass (leaves) during the dry periods because they are rich in protein and carotene. Le Houerou (1992) indicates that A. halimus can survive under rainfalls of 100-400mm per year . A. halimus is used as a means of combating desertification. Plants can fix atmospheric CO_2 following the C4 biosynthetic pathway. When excreting salt from the soil through its leaves, A. halimus becomes a potential desalination plant, provided the material is removed periodically to prevent the salt from returning. A. halimus is tolerant to intense and brief grazing, when it can fully recover the year after being grazed (Valderrábano et al., 1996; Falasca, 2013).

3. Methods

Four main actions were carried out to quantify the potential carbon sequestration that corresponds with the research questions of section 1.3. the actions and their integration in the final action of defining the spatially specific carbon sequestration (step 4) are outlined in Figure 7.

1: The Jordan Badia was classified into four categories indicating suitability for MWH. The classification was based on soil characteristics, water availability and slope. The three different shapes in Figure 7.1 represent different classes.

2: The optimal spacing between two neighbouring MWH pits was calculated. The spacing depends on rainfall, the runoff, the pit capacity and the yearly amount of water. The optimal spacing directly determines the area of land that can be restored because only the soil in 'the pit' will be restored.

3: Climatic, soil and biophysical inputs were gathered in the literature, and with fieldwork activities, the RothC-26.3 model was run for two locations in the study area, one where MWH has been present for five years and the other at an untreated site. The model, RothC-26.3, calculates carbon turnover in the top 23 cm of the soil.

4: The suitability and optimal spacing were used to find the total amount of restorable area; with the results of the RothC-26.3 model, it was possible to estimate location-specific potential carbon sequestration amounts.

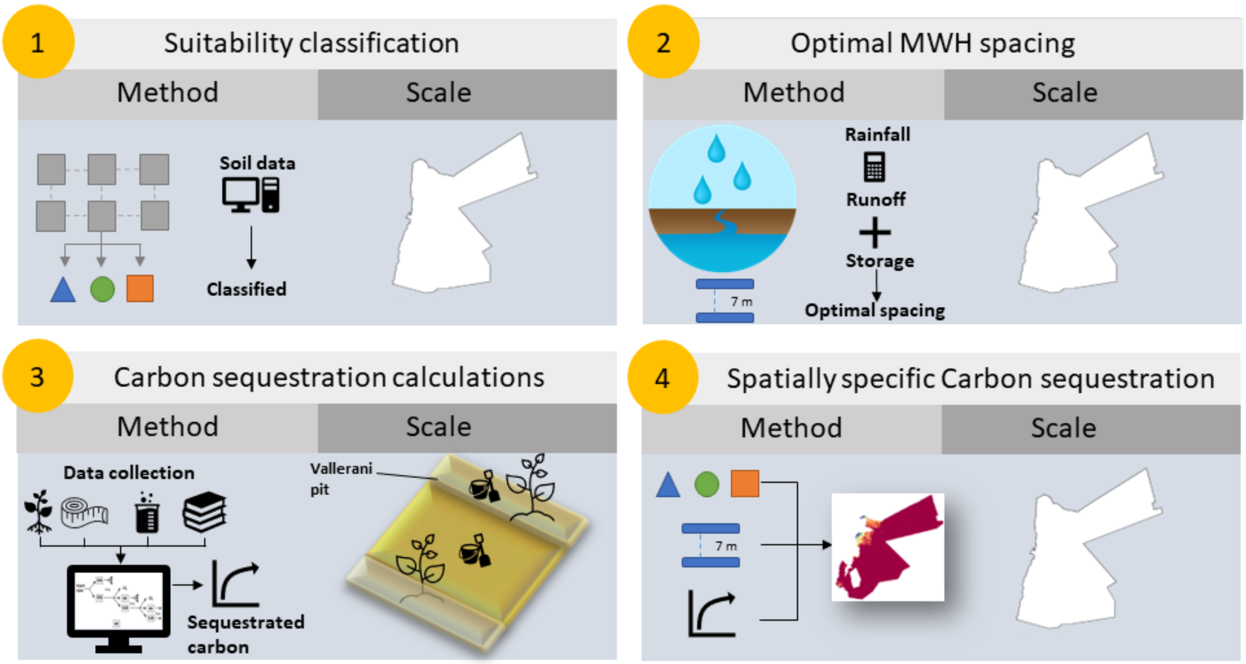

Figure 7 Schematic representation of the workflow of this study divided into four main actions. 1: Suitability classification, 2: Optimal spacing, 3: Carbon sequestration calculations and 4: Spatially specific carbon sequestration.

3.1 Suitability classification for MWH structures

3.1.1 Land suitability evaluation

For the successful restoration of degraded land, utilising the best conditions for vegetation development is essential. Vegetation development depends not only on the amount of rainfall, the effectiveness of water harvesting, and the suitability of the vegetation involved but also on the ability of soils to maintain good conditions for sustainable vegetation establishment. To find the areas in Jordan with the best conditions, a suitability classification has been performed where land is classified from highly suitable to unsuitable based on five properties (Figure 8): pH, clay content, cation exchange, average yearly rainfall and slope at the specific location. Clay content is the most crucial parameter to determine the soil's water-holding capacity which is essential for water availability. pH and cation exchange are relevant to soil health parameters indicating salinity and mineral level. The slope was also considered as MWH needs slope for runoff. Slope steepness is limited by a tractor's ability to create the structures. The above properties were specifically chosen because of their data availability for the Badia (and the world) and their relation to soil health.

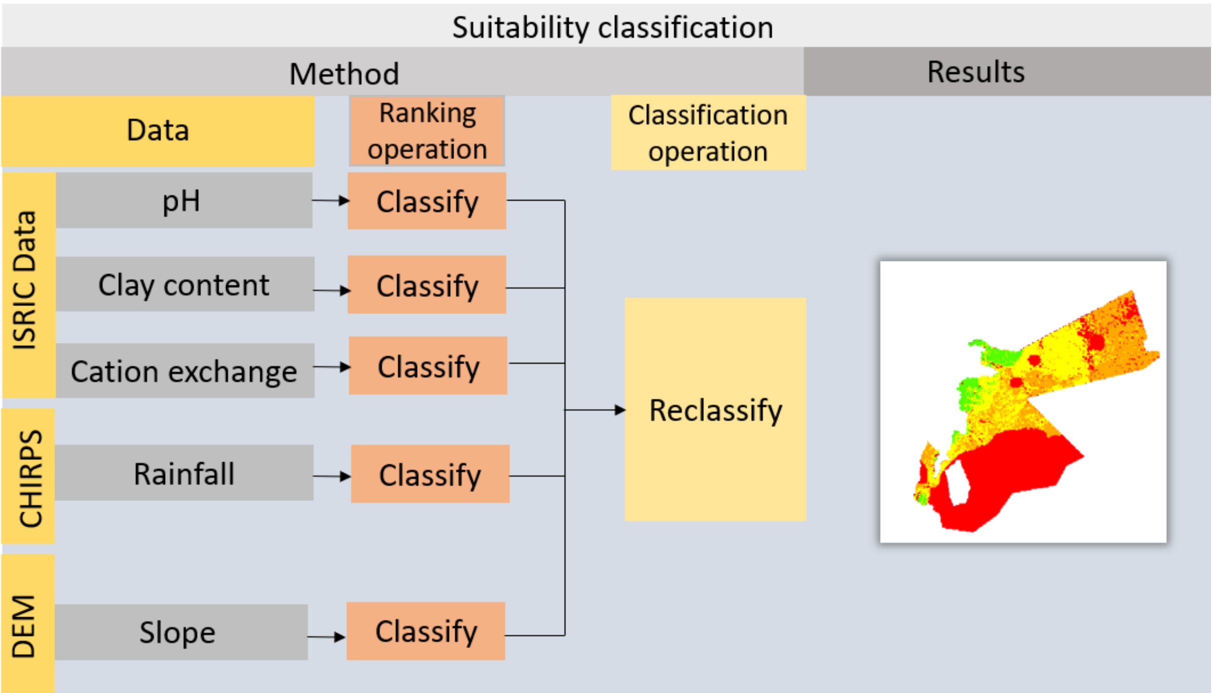

Figure 8 Flowchart of Land suitability evaluation. Data were processed to determine land suitability. The input is first ranked from low to high against several criteria and then consolidated. Data is then reclassified into the suitability map.

The evaluation of land suitability was approached with a ranking- and classification- system. First, for each property separately, all the areas in the Badia were ranked from least favourable conditions to most favourable (0 – 3); see 3.1.3 for the boundary values of the properties. Rainfall was ranked 0-6 because it was weighted twice due to its importance. Second, the areas were reclassified into four categories: highly suitable, moderately suitable, marginally suitable and unsuitable (Mazahreh et al., 2019). These categories indicate the potential for success for vegetation development when MWH is implemented. The categories are defined by the FAO as follows (FAO, 1983):

> ***Highly suitable***: Land that has no significant limitations for specified sustained use and is therefore expected not to reduce productivity or benefits or will not raise inputs above an acceptable level.
>
> ***Moderately suitable***: Land with moderately severe limitations for a specified sustained use. The limitations will reduce productivity or benefits and increase required inputs to the extent that the overall advantage of the use, although still attractive, will be appreciably lower than expected on class S1 land.

***Marginally suitable*:** Land with limitations that, in aggregate, are severe for sustained application of a given use and will reduce productivity or benefits, or increase required inputs, that this expenditure will be only marginally justified.

***Unsuitable* (NS)**: Land has limitations that appear severe to preclude any possible successful sustained use of the land.

3.1.2 Data relevance and availability

For the standard numerically defined soil properties (clay content, pH and Cation Exchange Capacity CEH), SoilGrids250m was used as provided by ISRIC (Batjes et al., 2017). Soilgrids is a global digital soil mapping system that uses machine learning to map the spatial distribution of soil properties across the globe. These 250 by 250-m grid resolution maps are globally defined and provide maps with parameters that are needed for this research (Hengl et al., 2017). ISRIC provides this data for seven depths: 0.00, 0.05, 0.15, 0.30, 0.60, 1.00, and 2.00 metres. The research was focused on topsoil. The averaged map of the four upper depths (up to 0.30 meters) was used for the suitability classification. For rainfall data, the CHIRPS dataset was used. CHIRPS (Climate Hazards Group InfraRed Precipitation with Station) dataset. CHIRPS incorporates satellite imagery with in-situ station data to create gridded monthly and daily rainfall time series with a spatial resolution of 0.05° by 0.05° (Retalis et al., 2017). Sarcinella (2020) did a sensitivity analysis and demonstrated that CHIRPS data provide reliable rainfall values for Jordan and is thus a reliable source for this study. The data includes daily rainfall from 1981 to the present. The rainfall data extraction was done for 2844 cells evenly spread across the Jordan Badia. The data was extracted from 01-01-1981 to 31-12-2021 (41 years), which was all available data. Yearly averages from 1981 to 2021 rainfall were used for this research.

3.1.3 Classification boundary values

For clay content, pH and rainfall, literature indicated the boundary values used (Krois et al., 2014; Falasca et al., 2013). Atriplex-specific values for cation exchange capacity were not found in the literature, so they were altered to create roughly evenly spread categories. Clay content, pH and cation exchange were ranked from 0-3; rainfall was weighted double and classified from 0-6, 3 (and 6) are highly-, 2 (and 4) moderately-, 1 (and 2) marginally- and 0 unsuitable. Table 1 lists the ranges of the characteristics corresponding to the four categories. The slope range is limited because slopes steeper than 25 degrees make it impossible for the tractor to make the MWH. For areas with almost no slope, ICARDA advises a different kind of land treatment, such as a Marab (Dhehibi et al., 2020).

Table 1 Properties classification boundaries for ranking suitability classes based on Krois et al. (2014) and Falasca et al. (2013)

Properties	*Highly suitable*	*Moderately suitable*	*Marginally suitable*	*unsuitable (NS)*
Clay content %	22.5-35	15-22.5	6-15 & 35-55	>55 & <6
pH [-]	7.2-7.9	7.0-7.2 & 7.9-8.0	6.5-7.0 & 8.0-9.0	
Slope (%)				25< & 0.1>
Cation exchange capacity (cmol/kg)	16.8-57.75	13.5-16.8	5.5-13.5	
Rainfall (mm/year)	> 250	250 - 200	200 - 150	< 150

3.1.4 Reclassification

All the data that were classified are consolidated and reclassified once again into the four FAO categories according to the following reclassification: an area with a score of 15-12 receives a highly suitable status, 11-9 a moderately suitable, 8-5 a marginally suitable, and regions with scores below 5 are identified as unsuitable for MWH. For better accuracy of the map, areas with a slope of 0 and areas with a soil depth smaller than 100 cm are excluded.

3.2 Optimal dimensions for MWH

Interspacing, the area between two pits, is essential to quantifying the effect of MWH structures. If the spacing (interspace) between two pits is oversized, it will collect too much runoff, fill its associated pit up and cause it to overflow, risking losing water and damaging the pits. Additionally, a larger interspace results in fewer pits, resulting in the less potential area in the pits for vegetation. On the other hand, if the interspace is too small, it will not collect enough water to meet the moisture demand of the vegetation. The optimum is where there is enough water for vegetation to grow, but the spacing is not too large to cause the risk of damaging the MWH structures. Therefore the 'minimum spacing', or the minimal distance between two structures, is calculated using runoff; see Figure 9 for a flowchart of this process. The runoff is related to the rainfall and soil type and was calculated using the Curve Number method (CN). The cumulative yearly volume can be determined by in- or decreasing the spacing at specific locations. This study calculates spacing for 200, 300 and 400 litres. Volumes were calculated for a spacing range between 4 and 25 metres. When spacing is smaller than 4 metres, the structures are too narrow for the tractor. If spacing is more extensive than 25 metres, the number of structures per hectare will be so low that MWH will not be feasible.

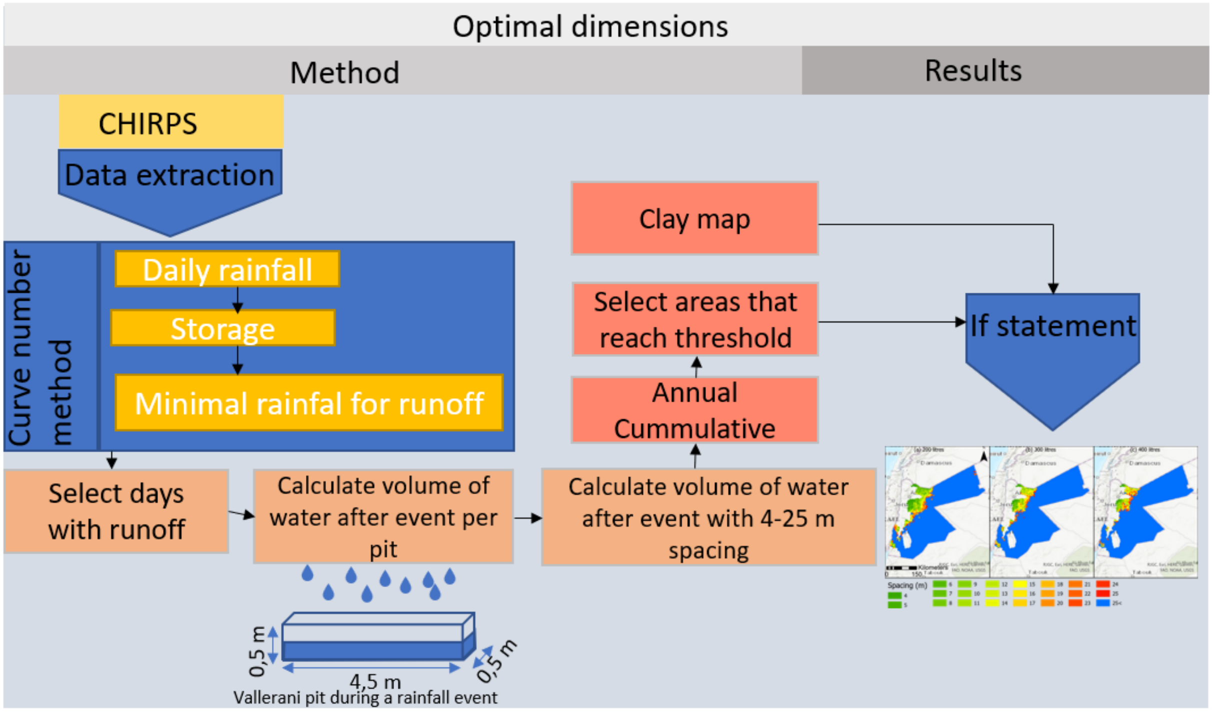

Figure 9 Flowchart for finding the optimum spacing. Rainfall data is extracted and used for the curve number method; then, the spacing is found using different steps

3.2.1 The curve number method (CN)

The CN is a method to calculate runoff using precipitation data and the curve number, describing the runoff potential per hydraulic soil group. (1) shows the equation of the CN:

$$Q = \frac{(P - Ia)^2}{(P - Ia) + S} \qquad (1)$$

Where Q is a runoff in cm, P is precipitation in cm, and I_a is an initial abstraction (2):

$$Ia = 0.2S \qquad (2)$$

S is the storage capacity of the soil which is calculated using (3):

$$S = \frac{25400}{CN} - 254 \qquad (3)$$

Where CN is the curve number determined by the soil type, the soil hydrological condition, vegetation cover, land use and treatment and the antecedent moisture condition (AMC) (I = dry, II = average, III = wet) of the soil (NCRS, 2004), this leads to (4):

$$Q = \frac{(P - 0.2S)^2}{(P + 0.8S)} \ (4)$$

If $P<I_a$, then Q is defined to be 0.

The CN ranges from 30 to 100; lower numbers indicate a higher rainfall threshold for runoff to occur, while higher numbers indicate lower rainfall thresholds for runoff potential. Different studies (Ali et al., 2010; Lesschen et al., 2009) showed that for crusty soils a rainfall runoff threshold of 4 mm is applicable. This study uses the CN method to calculate this rainfall runoff threshold (initial abstraction, I_a). The CN is related to soil type, soil infiltration capability and land use. This study is about runoff which only occurs in the wet season, so AMC(III) conditions were used.

3.2.2 Data availability

To use the CN method, two types of data were required. Rainfall data and the CN for all locations in de Badia. Daily rainfall data for the last 41 years were extracted from the CHIRPS data set (see 3.1.2). The CN was more complicated, as creating a CN map for the whole Badia was impossible due to lack of data availability (and time-wise did not fit into the scope of this thesis). The USDA Global CN map showed high values (97-99), which do not seem realistic for a desert because these values are more closely associated with an urban environment. Instead, in consultation with soil expert S. Strohmeier (March 2022), a more general approach was chosen for making a CN map. Al Majidiyya, the research site, has a CN of 86 and clay content of 33% (Shammout et al., 2018; Haddad et al., 2022). Considering that a higher clay content results in a higher CN, it was chosen to assign three different CNs to the Badia based on its clay content: 86 if clay content is between 30% and 35% (similar to the research site), 84 if it is below 30% and 88 when above 35%. 84 and 88 are educated guesses but are chosen to reduce complexity in the calculation process in the next step.

3.2.3 Calculating the spacing

To find the minimum spacing for each cell that is created, firstly, in MATLAB, the CN calculation was performed. This consisted of the following steps and was done for each of the CNs 84, 86, and 88:

- Calculate storage S and the initial abstraction for the CNs 84, 86 and 88.
- Calculate runoff Q for all 14975 days (41 years) on each of the 2844 locations.
- Filter out the days where $P<I_a$, and set Q to 0 for these days.
- Calculate the volume (V_1) of runoff that will originate on the surface area of one pit with a respective length and width of 4.5m x 0.5m. Note that this will be the amount of water that will enter the pit directly from rainfall that is, not via runoff.
- Calculate the volume of water that will enter a pit in one day: one calculation for each possible spacing between 4 and 25m. For example: to calculate the new volume (V_2) of water that entered a pit with a 7m spacing after a day of rainfall, one should multiply V_1 by 14 (because the width of the pit is 0.5m). See Figure 10.
- For each year at each location, sum the volumes and find the smallest spacing where runoff and direct rainfall in the pit reach the threshold (200-300- or 400 litres) for 30 out of the 41 years. The threshold of 300L is proven to be successful in the research site. The 200L and 400L thresholds are used for comparison.

Each location was assigned the correct minimum spacing using the CN map.

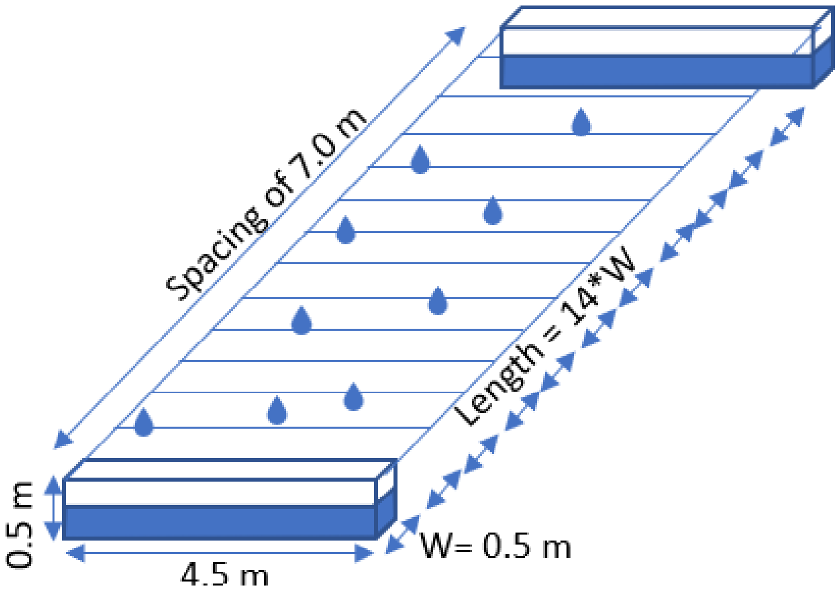

Figure 10 Example plot for calculating the spacing between two structures. A spacing of 7m has 14 times the width of one pit

3.3 Potential vegetation growth potential and carbon sequestration.

To model Soil Organic Carbon (SOC), Rothamsted Carbon 26.3 (RothC-26.3) was used (Coleman and Jenkinson, 1996). RothC-26.3 is a model that simulates the sequestration of organic carbon in topsoil. The model was previously used in the study by Hall (2019). For consistency, this follow-up study also used the model to calculate the total organic carbon turnover for a period of 20 years to present-day. To improve the results, a field study is carried out to find the initial TOC values in and next to an MWH pit when the study is conducted (January 2022). Figure 11 shows the flowchart of this process.

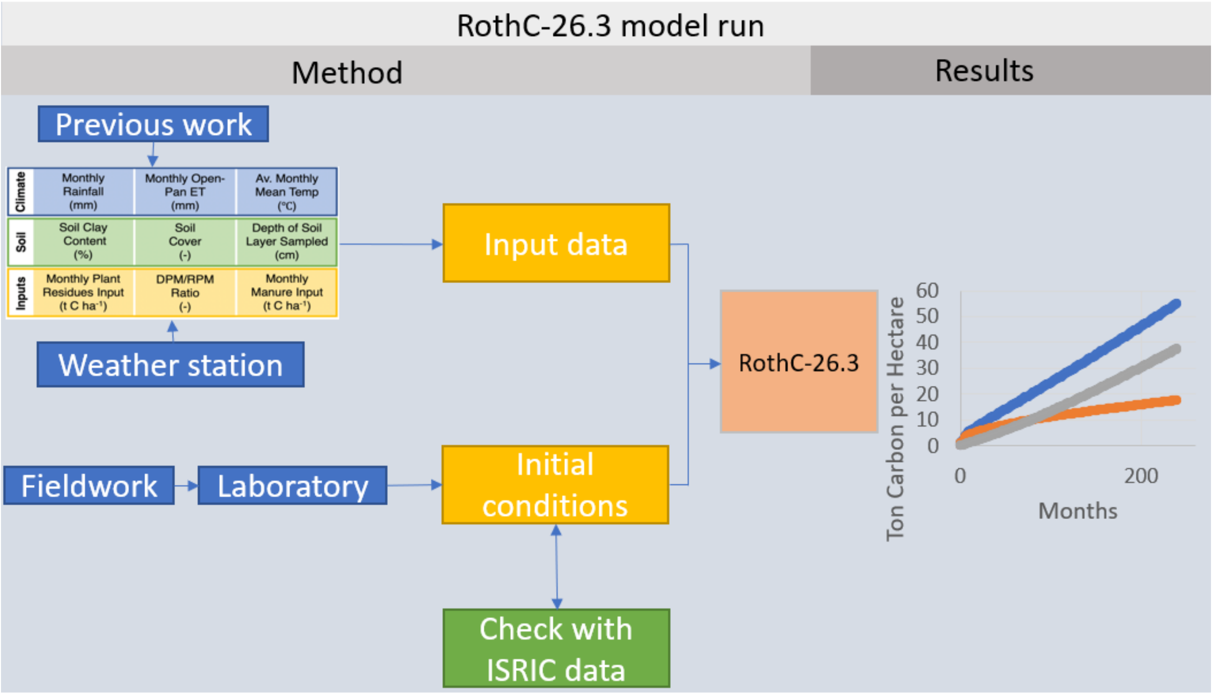

Figure 11 Flowchart for finding sequestrated carbon per hectare in the pit and the interspace

3.3.1 Runs

The model was run for two types of locations: location 1 is in the pit, and location 2 is in the interspace (Figure 12). At location 1, an MWH pit is made and resembles the treated situation where the soil is expected to improve. Location 2 resembled non-treated areas and was used to compare the change in carbon sequestration. More information about the specifics of the location can be found in 3.3.6 field experiments.

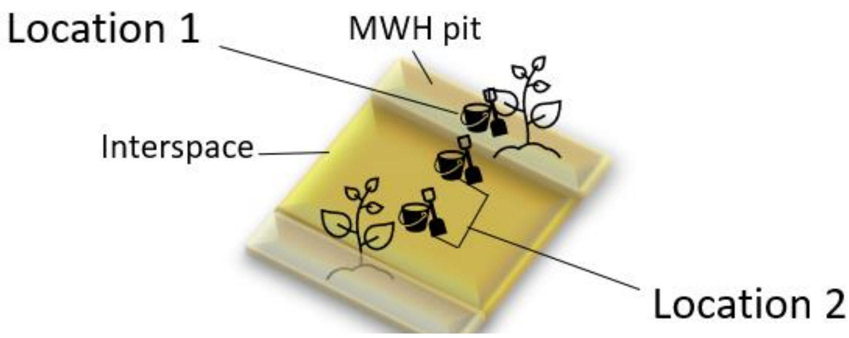

Figure 12 Schematic overview of sample locations

3.3.2 RothC-26.3 model

The RothC-26.3 model (Coleman and Jenkinson, 1996), a tool developed for predicting the dynamic evolution of the content of Soil Organic Carbon (SOC) under the effect of weather conditions and land use data, was used. A discrete dynamic model calculates SOC in monthly steps using steady-state data. Figure 13 illustrates the structure of the RothC-26.3 model. Organic input is split into decomposable and resistant plant material, and decays into CO_2, microbial biomass and humified organic matter. These steps repeat themselves. The model requires three inputs: climatic, soil and biophysical. In addition, initial conditions need to be set. The model calculates Total organic carbon (TOC), microbial biomass, and carbon age. TOC is calculated as the sum of the carbon contained in the above-ground biomass, carbon stored in below-ground biomass (e.g., roots) and SOC. The inputs were collected in the study area (3.3.1.3 field sampling) or were taken from earlier applications in this study area (Akimoto, 2020; Hall, 2021).

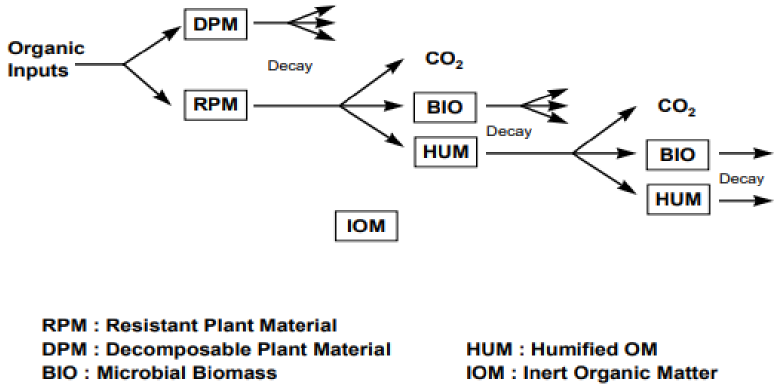

Figure 13 Model structure of RothC-26.3 model from Coleman and Jenkinson (1996). Organic inputs split into DPM and RPM.

3.3.3 RothC-26.3 model description

The amount of material in a soil layer Y that decomposes in a particular month is calculated by (5):

$$Y\, e^{-abck}\, t \qquad (5)$$

Where a is the rate modifying factor for temperature and is given by (6):

$$a = \frac{47.91}{1+e^{\left(\frac{106.06}{T+18.27}\right)}} \qquad (6)$$

Where T is the average monthly air temperature in °C.

b, the topsoil moisture deficit (TSMD) rate modifying factor for the moisture is calculated in the following way: First, Max TSMD for the top 23 cm layer of soil is calculated by (7):

$$Maximum\ TSMD = -(20 + 1.3(\%clay) - 0.04(\%clay)^2) \qquad (7)$$

Next, the accumulated TSMD for the specified layer of soil is calculated from the first month when 0.75 x (open pan evaporation) exceeds rainfall until it reaches the max TSMD, where it stays until the rainfall starts to exceed 0.75 x (open pan evaporation) and the soil wets up again. Because open pan evaporation is unknown, potential evapotranspiration can be used (Jenkinson, 1996). Note that the model is presently tuned to run on open-pan evaporation data, multiplied internally by 0.75 to give evapotranspiration. Data should therefore be divided by 0.75 before entering.

The maximum TSMD found is under actively growing vegetation during the growing season. If the soil is bare, this maximum is divided by 1.8, the BareSMD, to account for the reduced evaporation from bare soil. When the soil is bare, it is not allowed to dry out further than BareSMD unless the accumulated TSMD is already less than BareSMD, which cannot dry out any further. Finally, the rate modifying factor (b) is calculated:

$$If\ acc.TSMD < 0.444 * max.TSMD,$$
$$b = 0$$
$$otherwise,$$
$$b = 0.2 + (1.0 - 0.2) * \frac{max.TSMD - acc.TSMD}{max.TSMD - 0.444 * max.TSMD} \quad (8)$$

c is the soil cover rate modifying factor. When growing plants are present, decomposition is slowed.

$$If\ soil\ is\ vegetated \quad c = 0.6$$
$$If\ soil\ is\ bare \quad c = 1.0$$

k is the decomposition rate constant for that compartment. The decomposition rate constants (k) were initially set by Jenkinson (1996) on data from long-term field experiments (Table 2).

Table 2 Decomposition rates for the RothC-26.3 model by Jekinson (1996), see Figure 7 for explanations of abbreviations.

compartments	*Rate*
DPM	10.0
RPM	0.3
BIO	0.66
HUM	0.02

t is 1/12 since k is based on a yearly decomposition rate.

Both DPM and RPM decompose to form BIO and HUM as well as CO_2 in the first stage, with proportions controlled by the clay content of the soil. The ratio of CO_2/(BIO+HUM) is calculated using equation 9. Abbreviations are explained in Figure 7.

$$\mathrm{x} = 1.67\ (1.85 + 1.60\ \exp(-0.0786\ \%\mathrm{clay})) \quad (9)$$

Where x is the ratio of CO_2/(BIO+HUM).

x/(x+1) is then evolved as CO_2 and 1/(x+1) forms as BIO + HUM.

The BIO + HUM portion is divided into 46% BIO and 54% HUM. The model adjusts for clay content by altering the ratio between CO_2 and BIO+HUM. The relation between clay and BIO + HUM is shown in Figure 14.

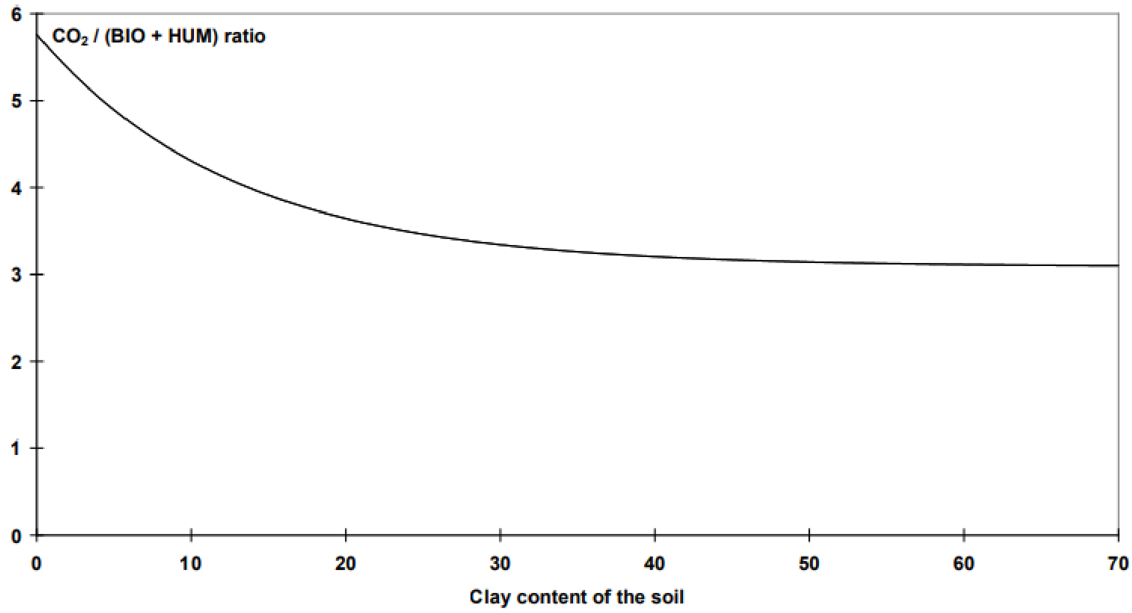

Figure 14 The effect of clay on the ratio of CO_2 released to (BIO + HUM) formed

3.3.4 Model input

The model requires three different types of input and a few initial conditions. In total, nine different inputs are needed (Table 3). The values used in the model can be found in appendix 1.

Table 3 RothC-26.3 data requirements according to Coleman and Jenkinson (1996)

Climate	Monthly Rainfall (mm)	Monthly Open-Pan ET (mm)	Av. Monthly Mean Temp (°C)
Soil	Soil Clay Content (%)	Soil Cover (-)	Depth of Soil Layer Sampled (cm)
Inputs	Monthly Plant Residues Input (t C ha^{-1})	DPM/RPM Ratio (-)	Monthly Manure Input (t C ha^{-1})

3.3.3.1 Climatic data

The starting climatic inputs are monthly precipitation and temperature and were derived from a weather station situated next to the Al Majidiyya research field at the Queen Alia International Airport. ICARDA calculated the monthly evapotransporation (ETo). ETo was divided by 0.75 to transform into open pan evaporation (Figure 15). This data is compared with the Climate Change Knowledge Portal and verified for consistency.

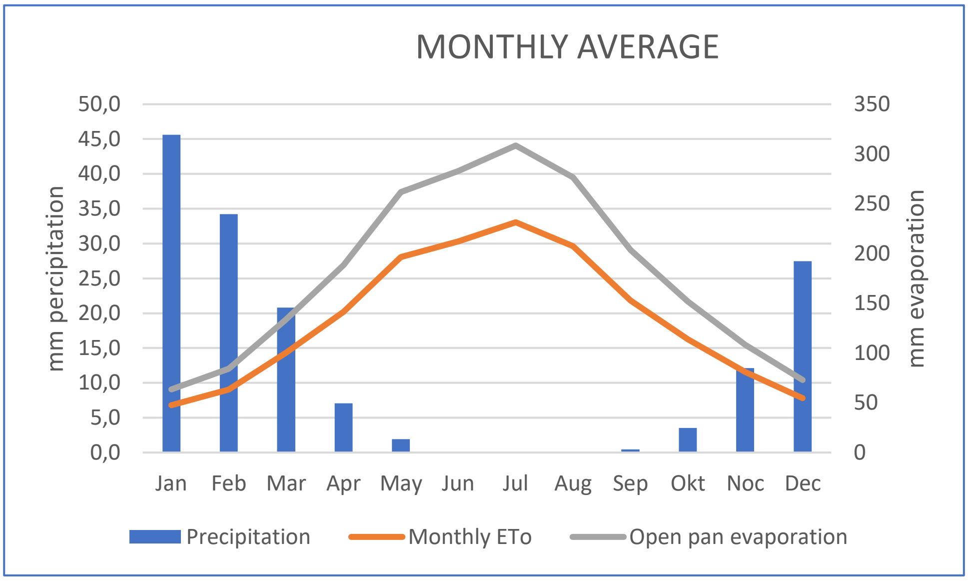

Figure 15 Climatic data of the Queen Alia International Airport weather station from 2010-2021 provided by ICARDA, including Precipitation monthly ETo and open pan evaporation.

3.3.3.2 Soil and remaining data inputs.

For the soil input, the clay content is taken from Haddad (2022) and is 33%. Soil cover is bare for half of the time for the interspace location (April – September). During the growing season, the soil is covered with annuals. The pit itself is covered from January until September. Plant residues are taken from former field studies in the research site by Akimoto (2020). The depth of the soil layer is the top 23 cm of the soil and is defined as the topsoil layer (Coleman and Jenkinson, 2014).

The DPM/RPM ratio links to the environment. In the case of unimproved grassland and shrubs, a DPM/RPM ratio of 0.67 is advised by (Coleman and Jenkinson, 2014). Monthly manure is calculated by the study by Hall (2021) as follows: goat manure typically contains 250g of carbon per 1kg, and a single animal produces between 0.37 and 0.38kg of manure per month in the wet season (Osuhor et al., 2002). An estimated ten goats graze per hectare around the field site, mainly from October to December. An observation in the field was that most of the manure is washed into the pits. Average manure input to the Vallerani furrow for a given month is therefore calculated from (10), and the result is converted from kg C ha^{-1} to t C ha^{-1};

$$Monthly\ input\ (kg\ C\ ha^{-1}) = \left(\left(amount\ of\ goats * monthly\ manure(kg) \right) * 0.25 \right)\ (10)$$

3.3.5 Initial conditions

Besides the inputs, the RothC-26.3 model requires initial conditions to calculate the carbon turnover. These consist of the start year (2022), the number of years the model is to be run (20), the number of years monthly output is required (20), and the initial soil carbon and radiocarbon values of each pool. The pools are Resistant Plant Material (RPM), Decomposable Plant Material (DPM), Microbial Biomass (BIO), Inert Organic Matter (IOM) and Humified Organic Matter (HUM). A sensitivity analysis was performed in the study by Hall (2021) to find the relative importance of each pool. The result showed no significant difference in the model's output when initial carbon was divided into five equal parts or increasing any of the fractions by 30%. So, in this study, equal fractions were used for the total initial carbon pools. The total carbon pool or TOC is found by sampling soil monsters in the field and analysing them in the laboratory using the Walkley-Black method (Mylavarapu, 2014). See 3.3.6 for field sampling. From the laboratory results, outliers were removed.

3.3.6 Field sampling

For the model, field data is collected to improve input as much as possible. During the data collection, the focus was on finding TOC in the soil and clay percentage. First, a general survey was conducted to find information about the current vegetation, using plant height, the diameter of the shrub (two directions), and stem diameter at the base of the plant.

In Al Majidiyya, 390 plants (+/-10% of the population) were measured for plant height, stem diameter, width, health status, and grazing status. By comparing the results in box-and-whisker plots, boundaries for the suitability classes were made. These boundaries were used for classifying all plants into three classes, from healthy to least healthy. To find the soil texture, samples were measured at 5 and 15 cm depth of the soil to indicate the topsoil. The clay percentage is found by measuring it in the laboratory with the hydrometer method (Haluka et al., 2014).
Initial total organic carbon (in t C/ha) inputs were found in the laboratory using the Walkley-Black method (Mylavarapu, 2014).

3.3.7 Field experiments

Class boundaries were found by conducting field measurements. The data was transferred into boxplots shown in appendix 1. The interquartile ranges of the boxplots are the boundaries of the classes. The average of two boundaries is taken as the boundary value of the plots with overlapping values. Class 1, the healthiest in the field, has the largest volume and class 3 the smallest. In figure 14, the fieldwork area is classified using the field data. The most significant part of the fieldwork area is classified in class 1. The lower classes are found towards the edge of the site, where soil depth is shallower. These classes were used to classify plants in the field, so when doing the other field measurements, it was clear which pits were needed to make a reliable image of the fieldwork area.

At nine different locations, of which three were S1, three were S2 and three S3, soil samples were taken in the pit, next to the pit, and in the interspace at 5 and 15 cm depths to find TOC. This resulted in a total of 54 samples.

For each location (interspace, next to the pit and in the pit), using the whisker-and boxplot method outliers of the TOC samples were excluded from further calculations.

3.4 Location specific carbon sequestration

With the use of the spacing map the efficiency was calculated. The efficiency is the ratio 'pit' to 'not a pit' in a hectare. This was needed because only the areas where pits are present, carbon is sequestered. To find how much carbon potentially can be sequestrated in 20 years, the efficiency map, the results of the RothC-26.3 model and the suitability map were combined, (Figure 16). The result is a map showing how much CO_2 (in tons) can be sequestrated per hectare if MWH is applied to suitable areas in the Jordan Badia.

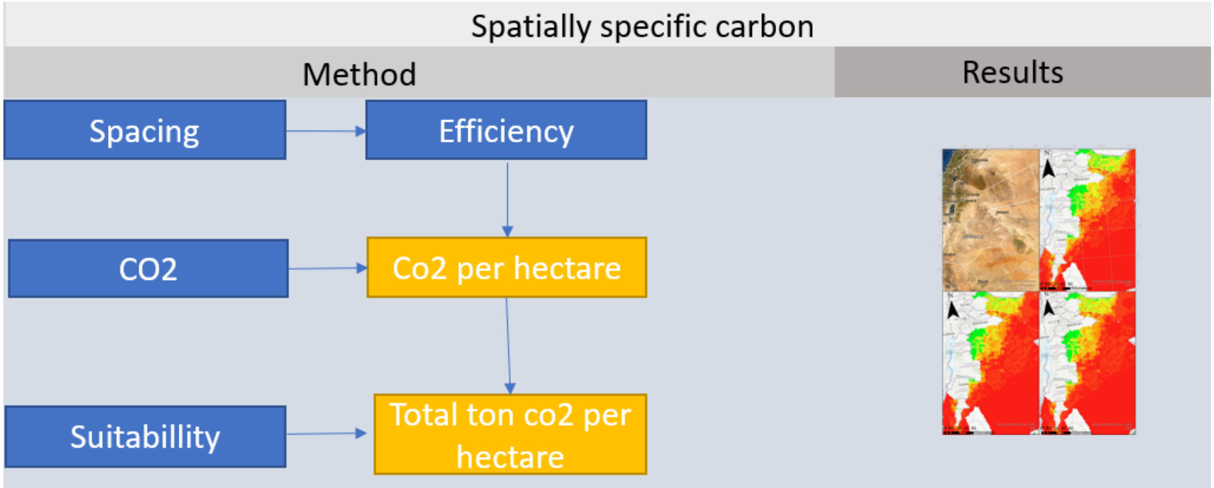

Figure 16 Flowchart of calculating the total amount of carbon sequestrated for the 200, 300, and 400 litre thresholds

3.4.1 Efficiency

The result of the model is given in metric tons of CO_2 per hectare. As only the turnover of atmospheric carbon takes place in the soil directly under the MWH pits, not all the areas where MWH is implemented contribute. To take this into account, an efficiency map was calculated. The efficiency indicates the percentage of a hectare used for sequestration. The efficiency was calculated by dividing 100 (the entire area) by the spacing. A treated area with an advised spacing of 7 meters will have an efficiency of 100/7=14.3%. If modelling results indicate that in 20 years in a pit, 50 tons of CO_2 per hectare would be sequestrated, the real value would be 7.15 tons of CO_2 per hectare, 14.3% of the original value.

3.4.2 Suitability

Areas are classified as highly suitable, moderately suitable, and marginally suitable. The classes stand for performance, so highly suitable areas will sequestrate more. Therefore, the classes will be associated with a success factor. Highly suitable is the top third and will succeed for 100-66%, moderately suitable 66-33%, and marginally suitable 33-0%. The average value of this success factor is used for further calculations. So, the classes received a success factor of 83%, 50%, and 17%, respectively.

3.4.3 Upscaling the modelling results

A map was created by multiplying the spacing map (efficiency), suitability percentages and the modelling results. pixels in these maps represent more than one hectare, so the value of each pixel is multiplied by the actual hectares per pixel. This last step was necessary to get the total amount of sequestered carbon.

4. Results

4.1 GIS approach for suitability classification

4.1.1 Land suitability evaluation

Figures 17 a-f show the ranked maps, and g and h show the reclassified maps. Figure 17a shows the pH. The most suitable areas are found in the West, while the East and the South-East have the least suitable areas. The middle is a combination of moderately and highly suitable. Figure 17b is the cation exchange capacity. The highest cation exchange, and thus the best circumstances are in the North-West and the North. The sizeable green patch in the North is a basalt plain which causes the high values. The North-East is presumably less suitable while the middle has alternating moderate and marginal conditions. Clay (Figure 17c) has declined, starting with clay percentages from 22.5 – 35% in the North-West and decreasing to below 22.5 in the South-East. The rainfall map (Figure 17d) has a similar pattern. The slope map (Figure 17e) did not exceed the maximum slope of 25 degrees. The areas excluded are all flat areas. The soil depth map (Figure 17f) did not discard any area. According to the ISRIC map, there were no areas where soil depth was less than 1 metre. This cannot be true as the Badia has a high rock cover and bedrock percentage, as visual interpretations demonstrate. In summary: the North-West area has the highest rainfall, pH, cation exchange, and clay percentages, resulting in the highest suitability. In the South-West, there is also an area with a high suitability classification due to high clay and pH values. In the North-East, areas marked marginally suitable result from low pH and cation exchange values. The middle of the Badia has an alternating pattern between marginally and moderately suitable caused by a low cation exchange capacity, a high pH and Clay percentage, and rainfall pattern that declines rapidly from high to low. The consolidation of these maps results in Figures 17-g and -h.

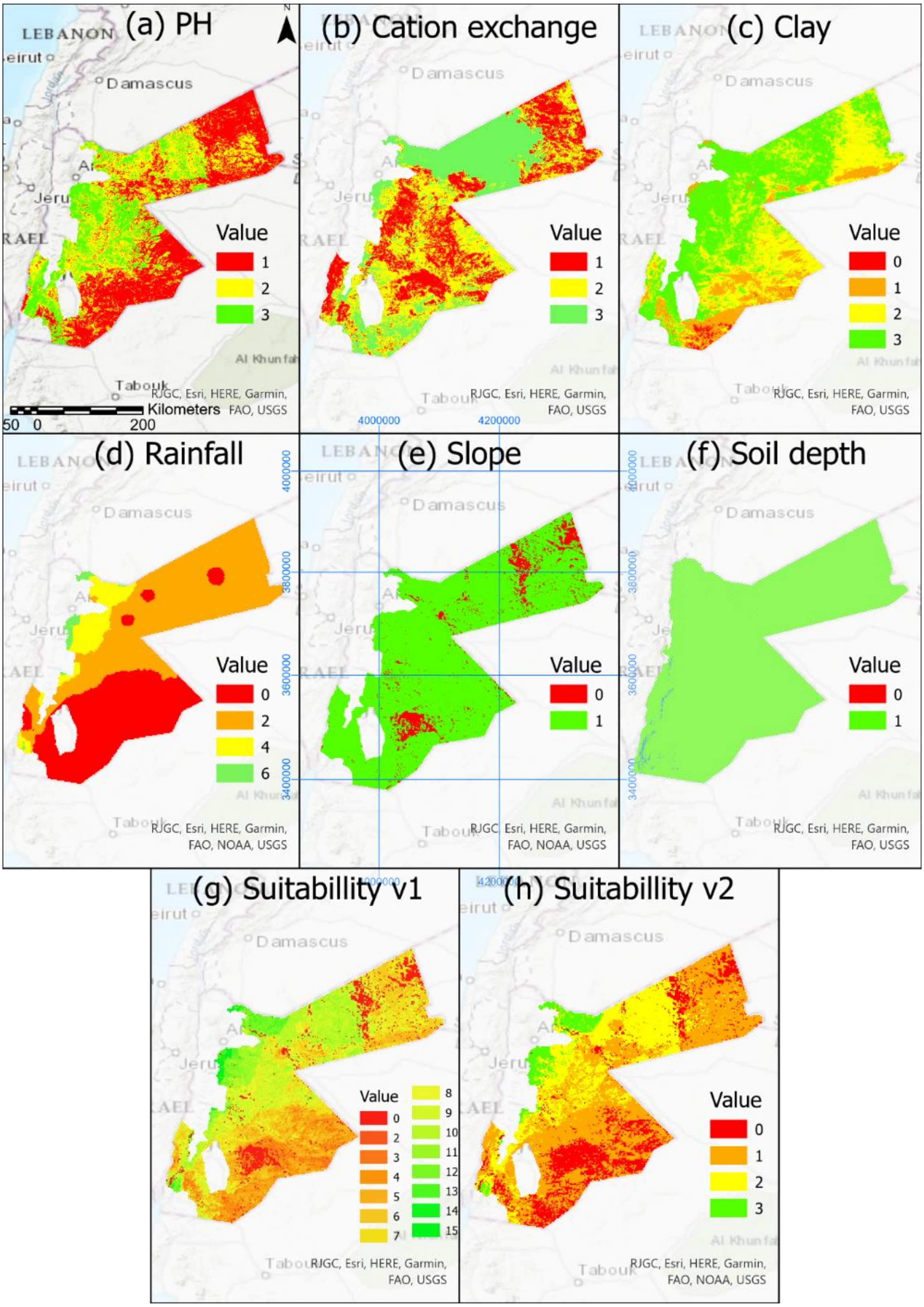

Figure 17a-h Inputs for suitability classification used for creating the suitability. Numbers indicate the order of suitability is 0 in an unsuitable area and 3, or 6 in case of rainfall, the most attributing area.

4.1.2 Reclassification to suitability map

In Figure 18, the result of the land suitability evaluation is shown. Results show that 42.5 per cent of the Badia is found to be unsuitable for MWH. 57.5%, on the contrary, is suitable: 24.5% marginally- 27.5% moderately- and 5.5% highly suitable. The highly suitable areas are primarily found in the North-West and along the West border of the Badia to the South. Highly suitable areas have the best biophysical and climatical conditions for MWH and seedlings are most likely to develop into healthy shrubs in these areas. The moderately suitable areas are in the North, centre and South-West of the Badia. Marginal areas are found in the North-East, East, centre, and South-West along the border with Israel. Generally, the map shows declining suitability from North to South and West to East, which is in line with the rainfall and clay percentage pattern. The South part of the Badia is classified as unsuitable. This area receives less than 100 mm of rainfall annually. In Figure 19, the raw pixel count of each class is shown. The pixel count was used for calculating the area belonging to each group. In the North a large area is categorised as moderately suitable while this area is comprised of basalt plains. The research area Al Majidiyya is classified as highly suitable.

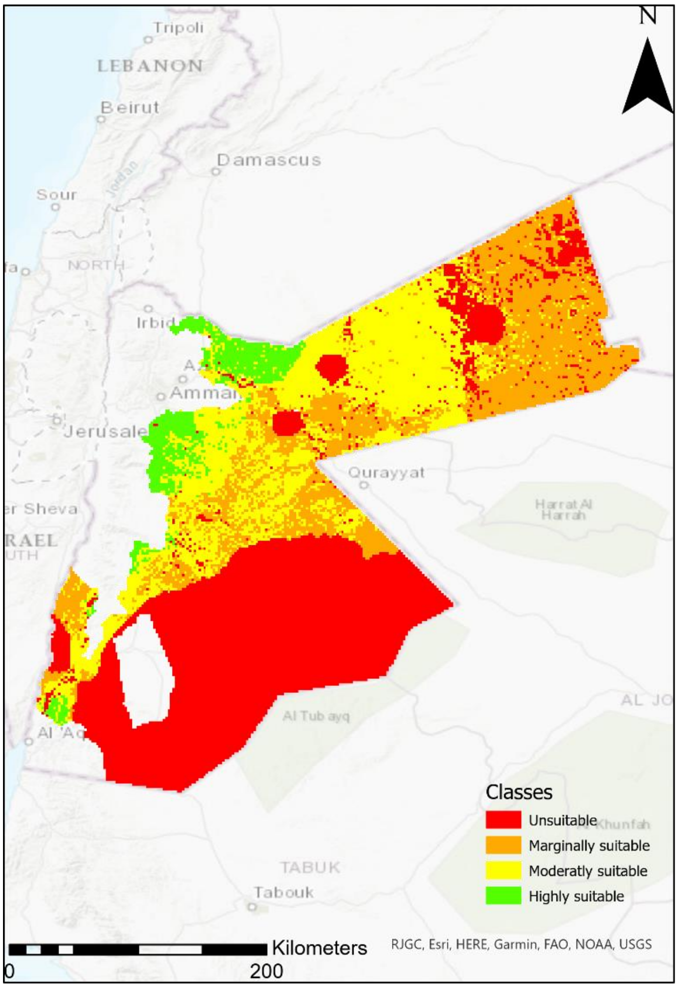

Figure 18 Land Suitability evaluation map classified into four classes: highly-, moderately-, marginally and, un-suitable.

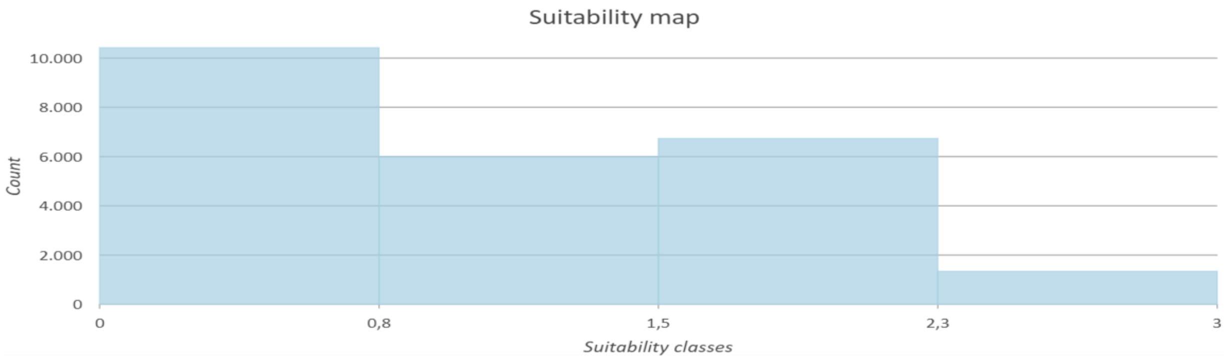

Figure 19 Pixel count of the four suitability classes. 0-0.8 is unsuitable, 0.8-1.5 is marginally suitable, 1.5-2.3 is moderately suitable, and 2.3-3 is highly suitable.

4.2 Optimal dimensions for MWH

For each of the 2844 rainfall extraction points, a curve number is assigned based on the clay percentage. The most significant part of the Badia is assigned the Curve Number value of 84 (Figure 20): areas that have a clay percentage lower than 30%. The North-West shows a small area of land with a CN of 88 (clay percentage higher than 35%), gradually going to 86 (clay percentage between 30% and 35%) and then to 84. The large area with CN 84 results in a lower overall runoff because soils with a lower CN have higher storage and initial abstraction values. The rainfall threshold for runoff generation was calculated to be 6.9 mm for a CN of 88, 8.3 mm for 86 and 9.7 mm for 84. 24% of the days that received rainfall had a total precipitation above 6.9 mm, 16% above 8.3 mm and 12.5% above 9.7 mm (figure 21).

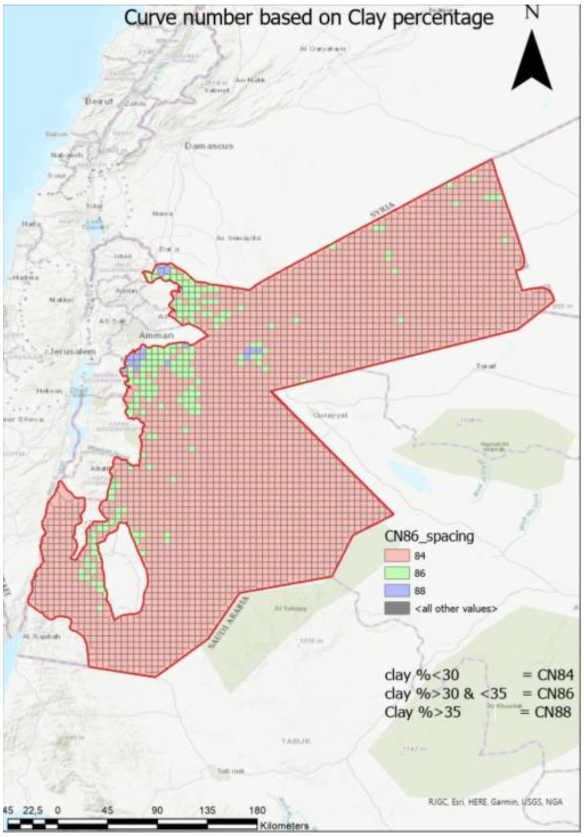

Figure 20 Curve number map, based on clay percentage

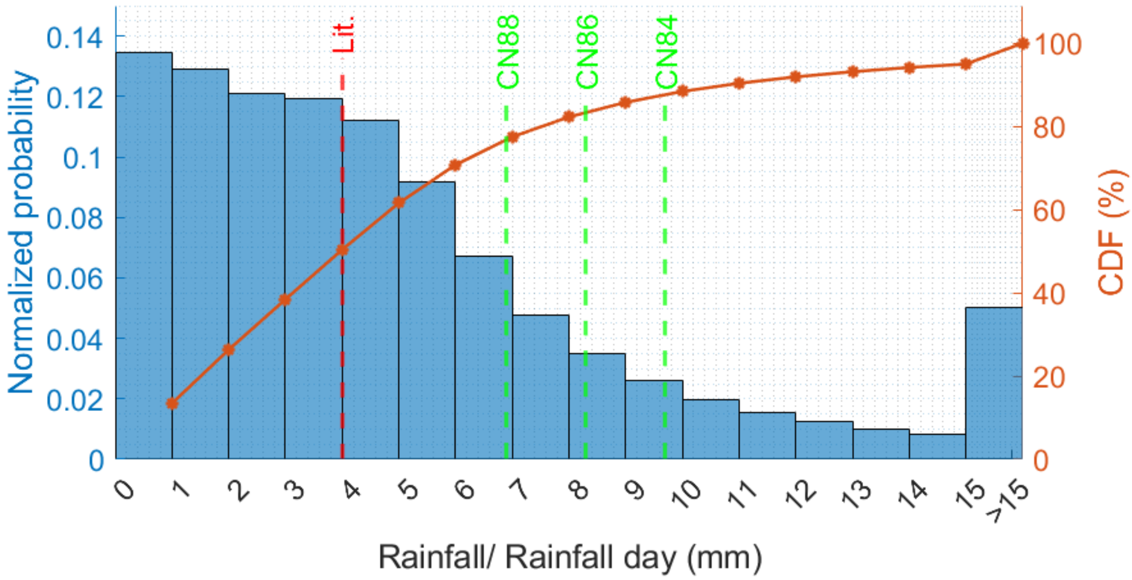

Figure 21 Normalized probability distribution of total precipitation on a day with rainfall. On the right y-axis the cumulative distribution frequency curve is displayed. 50% of the rainfall days receive more than 4 mm rainfall, 24% more than 6.9 mm, 16% more than 8.3 mm, and 12.5% more than 9.7 mm.

Figures 22a-c show the optimal spacing map of MWH structures in the Badia for threshold volumes of 200, 300, and 400 litres. The three maps show a similar pattern: small spacings and thus more MWH structures in the North-West and South-West along the Badia border. The spacing gradually increases towards the South and East until the thresholds cannot be reached anymore with consecutive MWH structures that have interspaces of 25 meters or smaller. With a 200 litre threshold, 16.5% of the Badia has a spacing below 25 metres, with 300 litres, 12.1%, and with a 400 litre threshold, it decreases to 9.5% of the land. This shows that lower thresholds increase the suitable area for MWH structures. The Spacing maps follow the same decreasing pattern as the suitability map but due to lack of runoff the usable area decreases drastically. Roughly, only the highly suitable area is suitable for MWH.

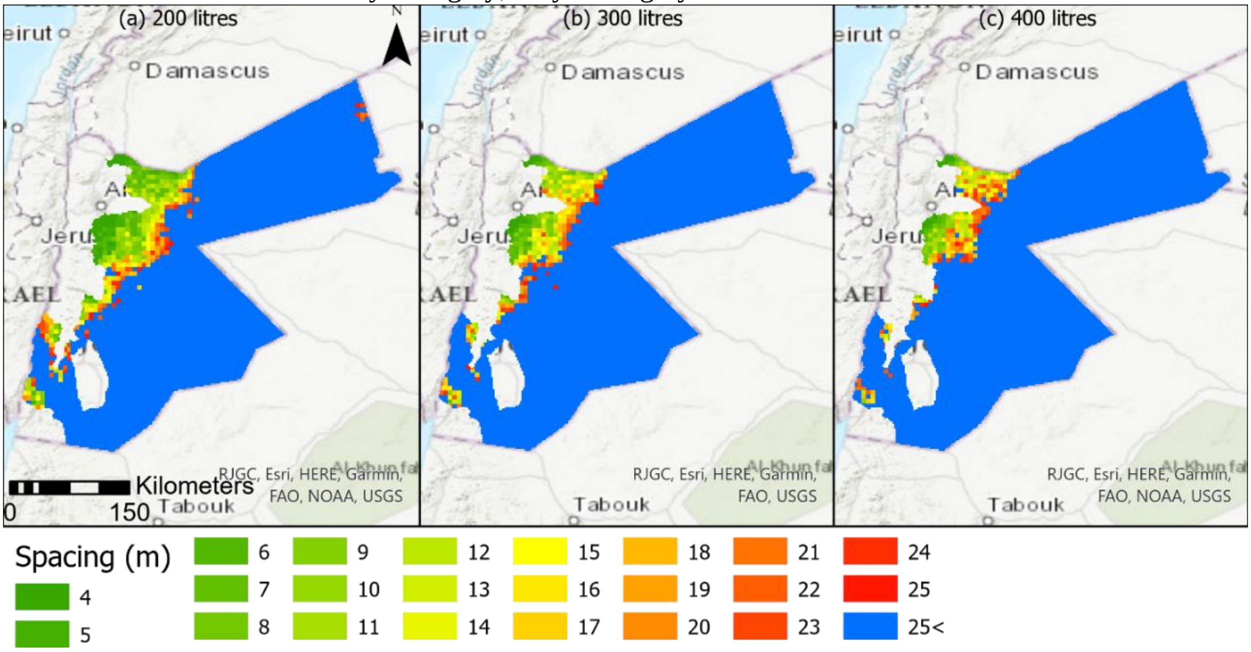

Figure 22 Spacing between two consecutive MWH structures in meters for a 200, 300 and 400 litre cumulative annual threshold.

Figure 23 displays the percent of area covered with the different spacings for the three thresholds. It shows that lower thresholds cause a relatively high percentage of area with smaller spacing (4-11 metres). The higher the thresholds, the more evenly distributed the spacings in the Badia. In general, it can be observed that rainfall (Figure 12-d) is the most determining factor for implementing MWH on a national scale in Jordan. Depending on the water needs of the vegetation, spacing can be adjusted so that yearly requirements are met.

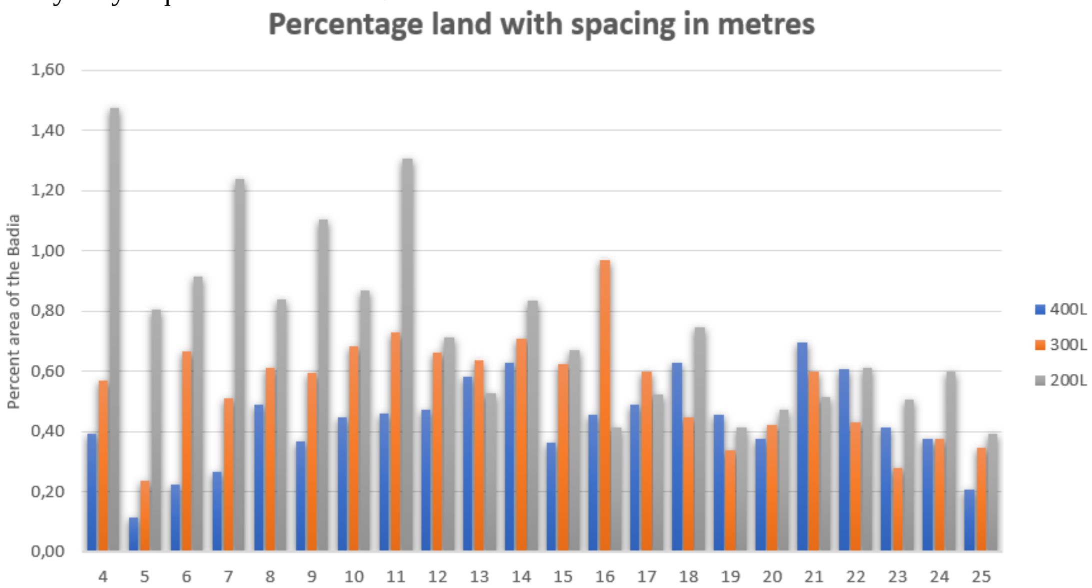

Figure 7 Percentage area of the Badia that potentially can be covered with MWH structures. Distinguished for 200, 30-, and 400 litre thresholds

4.3 Fieldwork results

Measurements of the 390 plants in the field are presented in whisker-box plots (Figures 24a-d). The 25 and 75 percentiles are shown and define the group boundaries where the 25 percentile is the lower boundary of the group and the 75 the highest boundary. When the 75 percentile of one group overlaps with the 25 percentile of another class (see Figure 24a), the average value of the two is taken as boundary value. The boundaries of the classes are shown in table 4 and the research area can be divided in these groups. In this table, class 1 has the shrub with the biggest volumes and 3 the smallest. Large volume shrubs are the healthiest shrubs.

Table 4 shows the boundaries of the classes.

Class	*1*	*2*	*3*
height	>95	95-65	65>
diameter	>1,5	1,5-1,1	1,1>
width 1	>125	125-75	75>
width 2	>115	115-75	75>

Figure 25 shows the research area, see Figure (1 or 2) for the location in Jordan, reclassified according to the new classes. This map is used for verifying the locations where TOC values were taken. Three MWH pits per class were chosen to take sample for TOC. These locations are indicated with a star on Figure 25.

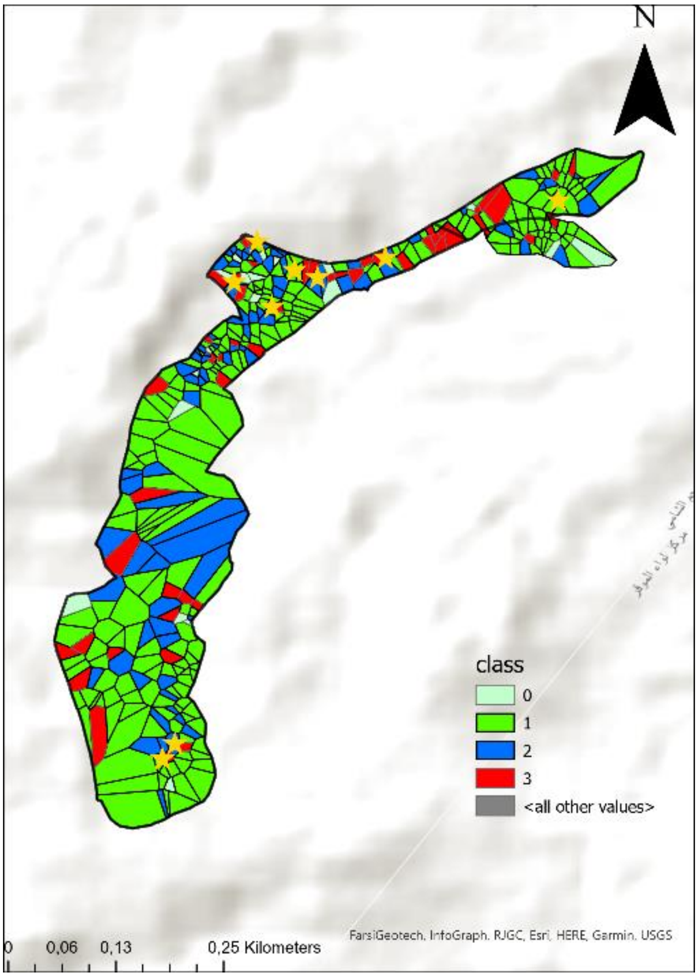

Figure 25 The research area divided according to the new boundaries. stars indicate locations where sampling has taken place

4.3.1 TOC calculations

The TOC sample outliers were removed using the whisker and box plots (Figures 26a-b). The samples removed are #20, #1 and #3, and #46. Table 5 shows the fractional TOC and the TOC in t/hectare which were converted using a bulk density of 1.38 g/cm^3 (Haddad et al., 2022); in the pit, the top layer has a TOC of 22 t/ha. This is an average of the top 5 cm and 15cm, which have weighted TOC values of 27.1 and 17.6 t/ha, respectively. The average 'not in the pit' value is 19.4 t/ha TOC. This is a combined average of the soil samples next to the pit and the soil sample of the interspace. The samples in the pit at 5 cm depth have an average value of 27 t/ha, which is higher than all the other values. The values of the not-treated areas range from 18-19.9 t/ha except for the 15 cm depth next to the pit; this is 16.5 and is noticeably lower than the surroundings.

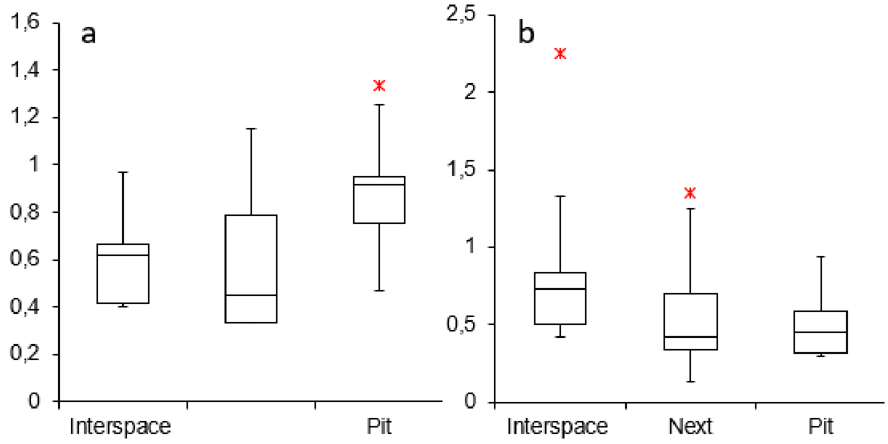

Figure 26 Box plots showing the TOC sample outliers for 15(a)- and 5(b)-centimetre depths

Table 5 TOC laboratory results

TOC%	*Average*	***5-cm***	***15-cm***
Average not pit	0.61	0.63	0.59
Average in the pit	0.69	0.83	0.55
average interspace	0.65	0.64	0.67
average next to the pit	0.56	0.61	0.52
TOC t/ha			
Average not pit	19.36	19.89	18.72
Average in the pit	22.04	27.06	17.57
average interspace	20.76	20.41	21.20
average next to the pit	18.05	19.37	16.55

4.3.2 Model results

The model calculated with monthly steps the TOC in tons per hectare for locations 1 and 2 (Figure 12) for a 20-year (240 months) period up to the present day (2022). Results are shown in Figure 27. Location 1 is in the pit, whereas location 2 is in the interspace and functions as a control plot that is not treated. Results from locations 1 and 2 are subtracted from each other to find the difference between treated and not treated. At location 1, after 20 years, 55.1 tons of carbon per hectare are sequestrated; at location 2, 17.5 tons of carbon per hectare are sequestrated. The difference between treated (in the pit) and not treated (interspace) is 37.6 tons of carbon per hectare according to the RothC-26.3 model. Figure 27 shows that CO_2 keeps increasing over the 20 years for both the 1 and 2 locations. When comparing locations 1 and 2, carbon sequestration occurs faster with treatment. After eight years, the carbon sequestrated carbon on location 1 is double that of location 2; after 20 years, it is tripled.

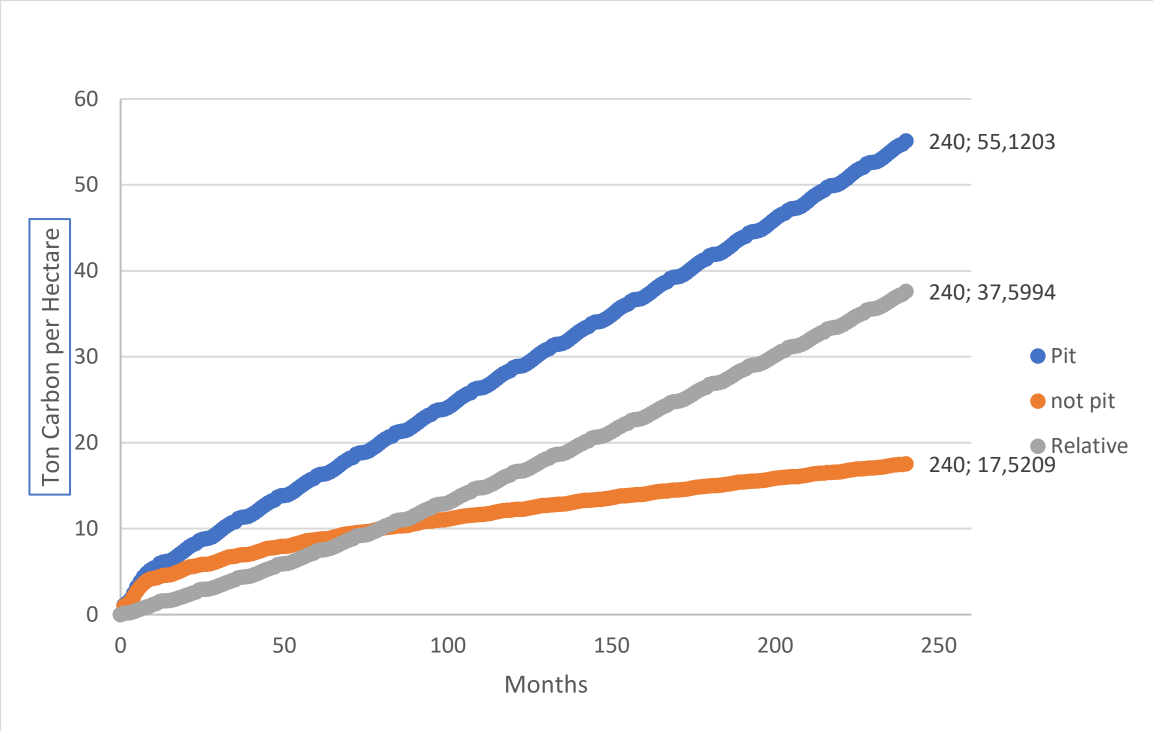

Figure 27 RothC-26.3 Model output. Sequestrated carbon in tons/hectare for locations 1 and 2. The grey line indicates the relative difference between locations 1 and 2.

4.4 Total Carbon per area

Using (11) sequestration values were calculated for the three thresholds.

$$Sequestration\ (per\ cell) = Model\ result * efficiency\ map * suitability\ map \quad (11)$$

With a threshold of 200 litres, 1105914 tons of CO_2 can be additionally sequestrated on 16.5% of the land in the Badia. A threshold of 300 litres results in sequestration of 815618 tons of CO_2. Furthermore, the 400 litre threshold sequestrates 480288 extra tons of CO_2 as opposed to no MWH implementation, which is captured on 9.5% of the Badia (Figure 28). Generally, the highest sequestration values (in tons of carbon per cell) are found in the North-West of the Badia, where spacing is the smallest and suitability is the highest. The pattern of the map is comparable with the spacing map. Spacing and rainfall are thus the most determining factor for the MWH. Vegetation that requiers lower thresholds, or other WH techniques can be used to increase the implementation area.

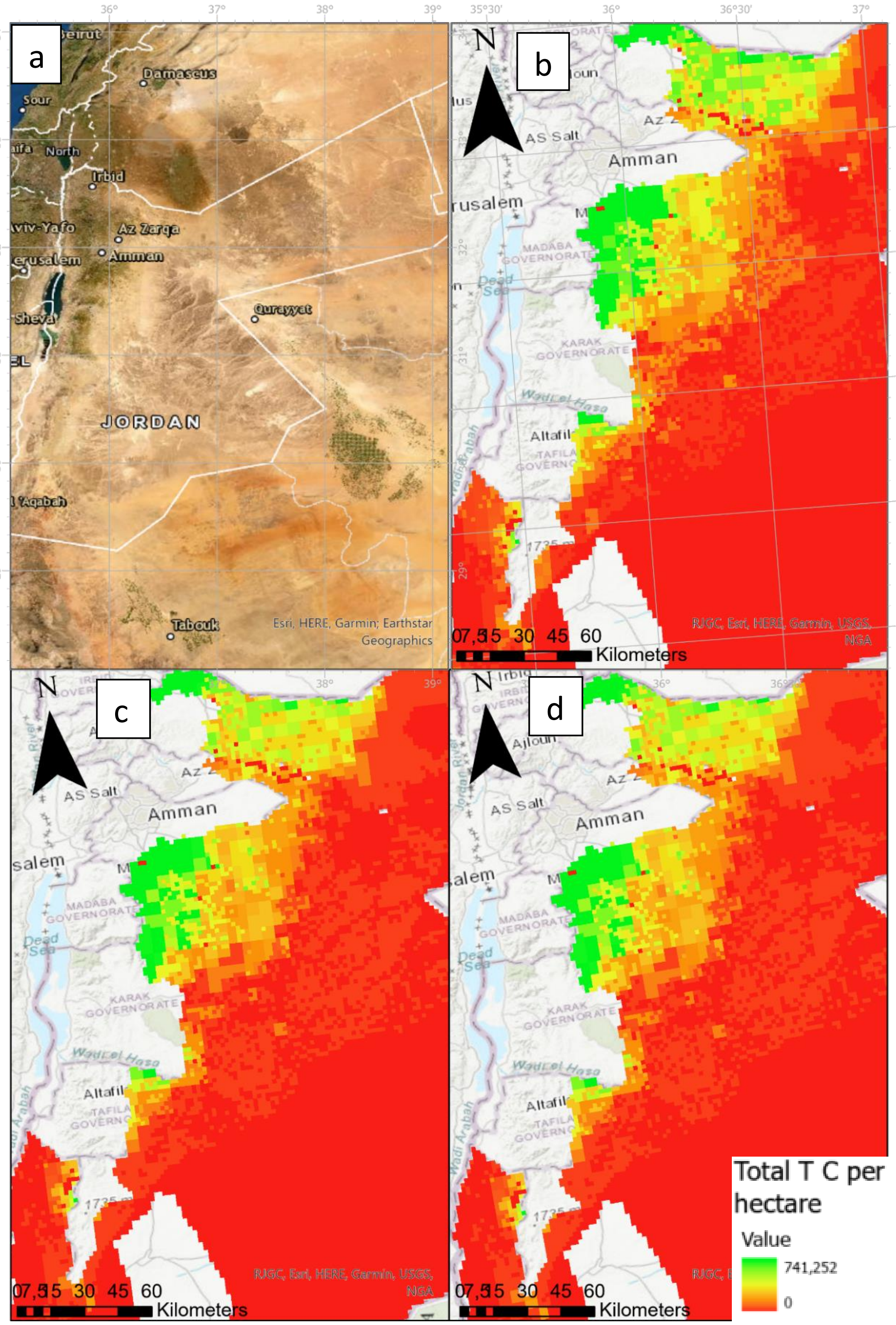

Figure 28 Aerial map of Jordan (a) and results from the map for 200(b), 300(c) and 400(d) litre thresholds. the result shows the total sequestrated area per cell

5. Discussion

Depending on the yearly amount of water desired for the A. halimus, 200, 300 or 400 litres, between 0.48 Mt and 1.1 Mt of carbon can potentially be sequestrated in 20 years by using Mechanised micro water harvesting (MWH) on a large scale in the Badia. This is a maximal 0.275% of Jordan's annual ~25 Mt annual carbon emissions (World Bank). Between 9.5 and 16.5% of the Badia is found suitable for the MWH based on the water availability; when looked at from a biophysical and climatical point of view, 57.5% is suitable, divided into three classes. The most suitable areas can predominantly be found in the North-West area of the Badia.

This study aimed to develop a method that improves the accuracy of quantifying the potential amount of carbon sequestration by up-scaling MWH to suitable areas in Jordan. The aim is reached by the following actions:

- classify the Badia into different suitability classes by conducting a land suitability evaluation
- find the density of MWH by defining the optimal spacing between two consecutive structures
- combine the above two with the results of the RothC-26.3 model run

The following section will discuss the results in terms of importance and influence on the primary research aim.

Suitability classification

Comparing the map of Hall (2021), which is displayed in Figure 3, and the land suitability evaluation (Figure 18), the location and size of the suitable area are generally consistent. There is one significant distinction between the North and North-East where the land suitability evaluation showed that the area is suitable. In contrast, Hall's map shows that these areas are not suitable. Hall's criteria, slope, soil depth, clay-, sand-, and stone- content and precipitation, were more directed to whether MWH is possible. At the same time, the land suitability evaluation of this study also looked at 'how' successful an area would be. The difference is made with the stone content and soil depth map. The North-East area consists of basaltic plains, which are seen as rocky and should be filtered out because MWH structures cannot be placed here as the plough will not be able to dig into the ground.

The suitability map is also visually compared with the study of Al-Shabeeb (2016), which used GIS to select potential water harvesting sites in the Azraq Basin in Jordan using the FAO classification. The maps have high similarity. The two studies use similar criteria for finding suitable areas, such as rainfall, clay content, and slope, but Al-shabeeb (2016) also incorporates drainage density, lineament density, and geology.

So, although the suitability evaluations in the different studies were made with different criteria but with three shared criteria: rainfall, clay content, and slope, the resulting maps showed a considerable resemblance. This invites the conclusion that the shared criteria are the most significant for making a suitability evaluation. The suitability map created in this study has the same level of refinement as the study of Al-Shabeeb (2016) but expands the scale to the entire Badia. This study compared with the study of Hall (2021), increases the refinement with de addition of the different suitability classifications.

Optimal dimensions

With the optimal spacing, an extra step is added to the study of Hall (2021). The spacing improves information about the number of MWH which can potentially be implemented and therefore is of significant value for decision-makers. The effect of different spacings has been researched in studies (Gammoh, 2013; Ali et al., 2010) but solely focuses on small-scale experiments.

With the addition of the spacing in the formulae, the suitable area with the land suitability evaluation reduces from 57.5% to 9.5-16.5%. The areas still suitable for MWH are those with a higher CN (and thus clay content) and rainfall, which is in the North-West Badia. The spacing is determined using two

inputs: the rainfall and the CN. The spacing depends on the number of years that water in a pit reaches the threshold. By setting these thresholds at 75% there was a significant decline in suitable area. The threshold ensures that the vegetation always receives enough water in the pits.
Another point is that the rainfall threshold for runoff generation was calculated to be 6.9 mm for a CN of 88, 8.3 mm for 86 and 9.7 mm for 84. 24% of the days that received rainfall had total precipitation above 6.9 mm, 16% above 8.3 mm and 12.5% above 9.7 mm. In other studies threshold (Ali et al., 2010; Lesschen et al., 2009) the rainfall threshold for the runoff was found to be around 4 mm for a similar soil and climate. 50% of all rainfall days receive more than 4 mm rainfall. This shows that reducing the rainfall threshold from 9.7 (CN 84), which is used for the most significant part of the Badia, to 4 mm – 37.5% more days are included in the study. These are the days when rainfall is between 4 mm and 9.7 and could significantly expand the area suitable for MWH.

RothC-26.3
The transformation from a barren landscape into one with vegetation has a 285% increase in SOC (Liu et al., 2017). The RothC-26.3 showed that, with the inputs used, the extra carbon sequestration doubles in eight years and almost triples in 20 years when areas get treated with MWH. Although these values percentage-wise agree with the findings of Liu et al. (2017), the absolute values seem high. While this study shows an increase of 37.6 t/ha, which is 1.5 t/ha per year, other studies have values between 0.2-0.5 t/ha per year (Wang et al., 2011; Lal, 2009).

Inputs for the model were partly taken from previous research (Hall, 2021; Akimoto, 2020), measured in the field and the lab or observed in weather stations and calculated. The essential initial SOC in the treated area was found to be 22.04 t/ha. This is an average from soil samples of 5 and 15 cm depth. The 5cm had a value of 27 t/ha, which is high compared with all the other sample points, while the 15 cm had 17.6 t/ha, which is lower than the values of other 15 cm depth soil samples locations. Two hypotheses could explain this, either five years is not enough to change SOC in the soil by growing shrubs, or because with the Vallerani, you dig out the top 50 cm of the soil and are sampling a soil sample of 65 cm below the soil surface which could have lower values than the top 15. The high SOC in the top 5 cm of the pit is probably a combination of organic matter, the turnover of organic matter, and the inwash of the most nutrient-full top layer of the interspace due to erosion by runoff. The untreated area has a SOC of 19.36 t/ha.

The study by Hall (2021) used remote sensing to determine the initial SOC and found a value of 16 t/ha. The ISCRIC Soil organic carbon stock map shows SOC values of 24 t/ha in the research area and 23 t/ha in the untreated references area just to the East of the research area. The mean SOC in Jordan is as low as 11 t/ha.

A more detailed SOC sampling study should be conducted to find the exact reason. Compared with the soil organic carbon stock in tons per ha in the top 30 cm map of ISRIC and the Global Soil Organic Carbon Map of the FAO, carbon stocks show values of around 24 t/ha, which could be seen as a good match between the results from the sampling. The untreated areas have 21-23 t/ha carbon stock values, slightly higher than those measured. Another point of discussion is that the model is run for a location where spacing is lower, and suitability is high. The value modelled for this location is then used for the whole Badia.

Uncertainties and recommendations

The study by Hall (2021), which this study has used as its backbone, used a more simpler method to calculate the extra carbon sequestration. That study showed that 51.2% of the Jordan was suitable for MWH and could store 3.0 Mt of carbon in 10 years, which is between 3 to 6 times more carbon sequestrated than found in this study in 20 years. Lal (2002) 's study estimated a yearly carbon sequestration potential of 0.2-0.4 Gt for the whole MENA region. Calculating this for Jordan, considering the surface area deemed suitable if 16.5% of the Jordan Badia, yearly carbon sequestration potential is 0.15-0.3 Mt per year, which is also 20-40 times more than the result of this study.

The developed method in this study provides a good roadmap for identifying where and how much carbon can be sequestrated. The information provides an overview for decision makers of which soils have the most significant potential for success after implementing MWH, either for using carbon sequestration, soil rehabilitation, or both.

The following recommendations are made. The focus on MWH implementation should be on highly suitable areas; these areas have a significant chance of successful MWH implementation. Comparison research needs to be carried out where other rehabilitation strategies need to be taken into account for areas that are marked as moderately, marginally and unsuitable. There is a chance that other techniques can rehabilitate these areas more successfully.

In hindsight, some further research is required to improve the quality of the method. Soil depth and a stone map are required for an accurate land suitability evaluation. More research needs to be done to the rainfall threshold for the runoff on crusty soils for finding the exact runoff in these degraded areas. Lastly, the long-term effects of MWH on carbon sequestration need to be researched in semi-arid and arid soils. So short and long-term carbon sequestration predictions can be made.
This study aims to improve the work of Hall (2021) by developing a method that can quantify the potential amount of carbon sequestration specific to any particular *location* when MWH is implemented.

6. Conclusion

This study was performed to refine the work of Hall (2021) by developing a method that can quantify the potential amount of carbon sequestration specific to any particular *location* when MWH is implemented. Jordan Badia was used as a case study. To achieve this aim, the following objectives were defined:

I) Classify the Jordan Badia into different suitability categories for MWH (and thus carbon sequestration) based on physical soil and climatical characteristics.

The Jordan Badia is divided into four suitability categories: Highly suitable, moderately suitable, marginally suitable, and unsuitable. Results show that 42.5% of the Badia is unsuitable for MWH. 24.5% marginally suitable, 27.5% moderately suitable, and 5.5% highly suitable. The divisions are made based on soil and climatical conditions. The suitability decreases from North to South and from West to East.

II) Determine optimal dimensions of the Vallerani MWH structures for successful plant growth based on the rainfall-runoff ratio.

To find the density of structure, the optimal spacing was calculated using the curve number method for an annual water threshold of 200, 300, and 400 litres; between 9.5 and 16.5% of the Badia received enough rainfall to meet these criteria with a spacing of 4 to 25 metres in between two consecutive structures. The decrease from 57.5% suitable area to 9.5-16.5% between RQ I and II are explained by the high rainfall runoff threshold and the method of selecting how much water is collected in a year. The areas with the smallest spacing and the highest densities were found in the North-West

III) Quantify potential location-specific carbon sequestration for the Jordan Badia.

The RothC-26.3 model showed that after MWH implementation, 37.6 tons of carbon per hectare could be sequestrated over 20 years. Combining this value with the spacing map and the suitability map, the result showed that between 0.48 and 1.1 Mt carbon could be sequestrated using MWH structures in the suitable areas of the Jordan Badia. The areas with the most impact are in the North-West, and its impact decreases from North to South and West to East.

With this study, a method has been created to select areas that are most amenable to MWH. Although the sequestration values do not reduce the impact of climate change significantly, they affect the Badia positively in multiple ways as the carbon increases the soil health, the plants trap more water, provide food for livestock, and rehabilitate the degraded soils.

For more accurate values, the relation between rainfall and runoff needs to be investigated for the different soils in Jordan. A reliable soil depth and stone map are required for a better suitability classification. A detailed study of the effect of carbon sequestration by vegetation on SOC is needed to increase understanding of the sequestration process.

References

Ababsa, M., 2013. Atlas of Jordan: History, Territories and Society. Presses de l'Ifpo, Institut français du Proche-Orient, Beyrouth, ISBN 9782351594384. https://doi.org/ 10.4000/books.ifpo.4560, 2013

Al-Alawi, M. T. (2008). Desertification in Jordan: A security issue. In *Environmental change and human security: recognizing and acting on hazard impacts* (pp. 81-102). Springer Netherlands.

Al-Homoud, A. S., Allison, R. J., Sunna, B. F., & White, K. (1995). Geology, geomorphology, hydrology, groundwater and physical resources of the desertified Badia environment in Jordan. *GeoJournal*, *37*(1), 51-67.

Ali, A., Yazar, A., Aal, A. A., Oweis, T., & Hayek, P. (2010). Micro-catchment water harvesting potential of an arid environment. *Agricultural Water Management*, *98*(1), 96-104.

Al-shabeeb, A. R. (2016). The use of AHP within GIS in selecting potential sites for water harvesting sites in the Azraq Basin—Jordan. *Journal of Geographic Information System*, *8*(1), 73-88.

Anschütz, J., Kome, A., Nederlof, M., Neef, R. D., & Ven, T. (2003). Water harvesting and soil moisture retention.

Batjes, N. H. (2006). Soil carbon stocks of Jordan and projected changes upon improved management of croplands. *Geoderma*, *132*(3-4), 361-371.

Batjes, N. H., Ribeiro, E., Van Oostrum, A., Leenaars, J., Hengl, T., & Mendes de Jesus, J. (2017). WoSIS: providing standardised soil profile data for the world. *Earth System Science Data*, *9*(1), 1-14.

Bulcock, L. M., & Jewitt, G. P. W. (2013). Key physical characteristics used to assess water harvesting suitability. *Physics and Chemistry of the Earth, Parts A/B/C*, *66*, 89-100.

Coleman, K., & Jenkinson, D. S. (1996). Roth-26.3-A Model for the turnover of carbon in the soil. In *Evaluation of soil organic matter models* (pp. 237-246). Springer, Berlin, Heidelberg.

de ROMERO, M. E. M. (1981). Contribuciones al estudio del género Atriplex (Chenopodiaceae) en la Argentina, I. *Darwiniana*, *23*(1), 119-150.

Delphin, S., Escobedo, F. J., Abd-Elrahman, A., & Cropper Jr, W. (2013). Mapping potential carbon and timber losses from hurricanes using a decision tree and ecosystem services driver model. *Journal of environmental management*, *129*, 599-607.

Dhehibi, B., Haddad, M., Strohmeier, S., & El-Hiary, M. (2020). Enhancing a Traditional Water Harvesting Technique in Jordan's Agro-pastoral Farming System. *International Center for Agricultural Research in the Dry Areas (ICARDA): Beirut, Lebanon*.

Dregne, H. E. (2002). Land degradation in the drylands. *Arid land research and management*, *16*(2), 99-132.

Droogers, P., Immerzeel, W. W., Terink, W., Hoogeveen, J., Bierkens, M. F. P., Van Beek, L. P. H., & Debele, B. (2012). Water resources trends in Middle East and North Africa towards 2050. *Hydrology and Earth System Sciences*, *16*(9), 3101-3114.

Falasca, S. L., Pizarro, M. J., & Mezher, R. N. (2014). The agro-ecological suitability of Atriplex nummularia and A. halimus for biomass production in Argentine saline drylands. *International journal of biometeorology*, *58*(7), 1433-1441.

FAO. Guidelines: land evaluation for rainfed agriculture. Food and Agriculture Organization of the United Nations, Soils Bulletin 52. Italy: Rome; 1983.

Franceschini, G., De Leo, E., & Muchoney, D. (2019). Jordan—Land Cover Atlas. *FAO: Rome, Italy*.

Freiwan, M., & Kadioğlu, M. (2008). Climate variability in Jordan. *International Journal of Climatology: A Journal of the Royal Meteorological Society*, *28*(1), 69-89.

Gammoh, I. A. (2013). An improved wide furrow micro-catchment for large-scale implementation of water-harvesting systems in arid areas. *Journal of arid environments*, *88*, 50-56.

Haddad, M., Strohmeier, S. M., Nouwakpo, K., Rimawi, O., Weltz, M., & Sterk, G. (2022). Rangeland restoration in Jordan: Restoring vegetation cover by water harvesting measures. *International Soil and Water Conservation Research*.

Hall, L (2021). Quantification of Soil Carbon Sequestration Potential in Dryland Micro-Rainwater Harvesting Structures (Master's thesis)

Hengl, T., Mendes de Jesus, J., Heuvelink, G. B., Ruiperez Gonzalez, M., Kilibarda, M., Blagotić, A., ... & Kempen, B. (2017). SoilGrids250m: Global gridded soil information based on machine learning. *PLoS one*, *12*(2), e0169748.

Huluka, G., & Miller, R. (2014). Particle size determination by hydrometer method. *Southern Cooperative Series Bulletin*, *419*, 180-184. 3959.

IPCC, 2014. Report Overview on climate Change 2014: Impacts, Adaptation, and Vulnerability. Part B. http://ipcc-wg2.gov/AR5/report/Natural Resources Conservation Service (NRCS). 2004. National engineering handbook: Part 630—Hydrology, U.S. Dept. of Agriculture, Washington, DC.

Jabri, B., & Hessane, M. A. (2020). Production of a Curve Number map using GIS Techniques in the watershed of the high Sebou (Morocco). In *E3S Web of Conferences* (Vol. 150, p. 03003). EDP Sciences.

Lal, R. (2002). Carbon sequestration in dryland ecosystems of West Asia and North Africa. *Land Degradation & Development*, *13*(1), 45-59.

Lal, R. (2009). Sequestering carbon in soils of arid ecosystems. *Land Degradation & Development*, *20*(4), 441-454.

Lesschen, J. P., Schoorl, J. M., & Cammeraat, L. H. (2009). Modelling runoff and erosion for a semi-arid catchment using a multi-scale approach based on hydrological connectivity. *Geomorphology*, *109*(3-4), 174-183.

Liu, X., Yang, T., Wang, Q., Huang, F., & Li, L. (2018). Dynamics of soil carbon and nitrogen stocks after afforestation in arid and semi-arid regions: A meta-analysis. *Science of the Total Environment*, *618*, 1658-1664.

Mazahreh, S., Bsoul, M., & Hamoor, D. A. (2019). GIS approach for assessment of land suitability for different land use alternatives in semi arid environment in Jordan: Case study (Al Gadeer Alabyad-Mafraq). *Information processing in agriculture*, *6*(1), 91-108.

Mulas, M., & Mulas, G. (2004). The strategic use of Atriplex and Opuntia to combat desertification. *Sassari, Italia: Desertification Research Group, University of Sassari*.

Mylavarapu, R. (2014). Walkley-Black Method. *Soil test methods from the Southeastern United States*, 158.

Osuhor, C. U., Alawa, J. P., & Akpa, G. N. (2002). Research note: Manure production by goats grazing native pasture in Nigeria. *Tropical Grasslands*, *36*(2), 123-125.

Oweis, T. Y. (2017). Rainwater harvesting for restoring degraded dry agro-pastoral ecosystems: a conceptual review of opportunities and constraints in a changing climate. *Environmental Reviews*, *25*(2), 135-149.

Retalis, A., Tymvios, F., Katsanos, D., & Michaelides, S. (2017). Downscaling CHIRPS precipitation data: an artificial neural network modelling approach. *International Journal of Remote Sensing*, *38*(13), 3943-

Reynolds, J. F., Smith, D. M. S., Lambin, E. F., Turner, B. L., Mortimore, M., Batterbury, S. P., ... & Walker, B. (2007). Global desertification: building a science for dryland development. *science*, *316*(5826), 847-851.

Roudi-Fahimi, F., Creel, L., & De Souza, R. M. (2002). *Finding the balance: Population and water scarcity in the Middle East and North Africa* (pp. 1-8). Washington, DC: Population Reference Bureau.

Schimel, D. S. (2010). Drylands in the earth system. *Science*, *327*(5964), 418-419.

Shawahneh, N., Saoub, H., Oweis, T., Haddad, N., & Karrou, M. (2011). Impact of microcatchment water harvesting on the diversity of the Badia rangelands of Jordan. *Rehabilitation and integrated management of dry rangelands environments with water harvesting*, 85.

Silvia Liliana Falasca & María José Pizarro & Romina Nahir Mezher, 2013

Sprong, C (2019). Soil water dynamics affected by micro rainwater harvesting structures in Jordanian Badia restoration context (Master's thesis)

Stockmann, U., Adams, M. A., Crawford, J. W., Field, D. J., Henakaarchchi, N., Jenkins, M., ... & Zimmermann, M. (2013). The knowns, known unknowns and unknowns of sequestration of soil organic carbon. *Agriculture, Ecosystems & Environment*, *164*, 80-99.

Strohmeier, S., Fukai, S., Haddad, M., AlNsour, M., Mudabber, M., Akimoto, K., ... & Oweis, T. (2021). Rehabilitation of degraded rangelands in Jordan: The effects of mechanized micro water harvesting on hill-slope scale soil water and vegetation dynamics. *Journal of Arid Environments*, *185*, 104338.

Statistics Do. Statistical Yearbook of Jordan 2019 [Available from: http://dosweb.dos.gov.jo/.

Sufardi, S., Arabia, T., Khairullah, K., Zainabun, Z., Karnilawati, K., & Sahbudin, S. (2020). Charge characteristics and cation exchanges properties of hilly dryland soils Aceh Besar, Indonesia. *Aceh International Journal of Science and Technology*, *9*(2), 90-101.

United nations (2011), Global Drylands: A UN system-wide response. Retrieved from https://www.unep-wcmc.org/resources-and-data/global-drylands--a-un-system-wide-response

Valderrábano, J., Muñoz, F., & Delgado, I. (1996). Browsing ability and utilization by sheep and goats of Atriplex halimus L. shrubs. *Small Ruminant Research*, *19*(2), 131-136.

van der Esch, S., ten Brink, B., Stehfest, E., Bakkenes, M., Sewell, A., Bouwman, A., ... & Mantel, S. (2017). Exploring future changes in land use and land condition and the impacts on food, water, climate change and biodiversity: scenarios for the UNCCD Global Land Outlook.

Wang, Y., Fu, B., Lü, Y., & Chen, L. (2011). Effects of vegetation restoration on soil organic carbon sequestration at multiple scales in semi-arid Loess Plateau, China. *Catena*, *85*(1), 58-66.

Westerberg, V., & Myint, M. (2014). An Economic Valuation of a large-scale rangeland restoration project through the Hima system within the Zarqa River Basin in Jordan. *IUCN, Nairobi*.

Zdruli, P. (2014). Land resources of the Mediterranean: status, pressures, trends and impacts on future regional development. *Land Degradation & Development*, *25*(4), 373-384.

Zhang, H., Wang, J. J., Sikora, F. J., & Moore, K. P. (2014). Loss on ignition method. *Soil test methods from the Southeastern United States. Southern extension and research activity information exchange group*, *6*, 155-157.

Zika, M., & Erb, K. H. (2009). The global loss of net primary production resulting from human-induced soil degradation in drylands. *Ecological Economics*, *69*(2), 310-318.

Appendices

Appendix 1 Inputs for RothC-26.3 model

scenario 1	Precipitation	Eto	Temperature	Clay	Cover	Soil depth	Plant residues	DPM/RPM	Manure
Jan	45,6	47,59853	7,931525	32,5	0,6	0,23	0,15	0,67	0,008438
Feb	34,2	63,18021	9,654705	32,5	0,6	0,23	0,15	0,67	0,008438
Mar	20,8	100,2235	12,59824	32,5	0.6	0,23	0,2	0,67	0,008438
Apr	7,1	141,2985	16,24455	32,5	0.6	0,23	0,25	0,67	0,008438
May	1,9	196,3626	20,911	32,5	0.6	0,23	0,3	0,67	0,008438
Jun	0,0	212,2946	23,40333	32,5	0.6	0,23	0,3	0,67	0,008438
Jul	0,0	231,4125	25,38035	32,5	0.6	0,23	0,3	0,67	0,008438
Aug	0,0	207,5142	25,36378	32,5	0.6	0,23	0,3	0,67	0,008438
Sep	0,5	152,6417	23,73377	32,5	0.6	0,23	0,3	0,67	0,008438
Okt	3,5	113,8375	19,83435	32,5	1	0,23	0,25	0,67	0,008438
Noc	12,1	81,14883	14,46483	32,5	1	0,23	0,25	0,67	0,008438
Dec	27,5	54,64711	9,425968	32,5	1	0,23	0,2	0,67	0,008438
scenario 2	Precipitation	Eto	Temperature	Clay	Cover	Soil depth	Plant residues	DPM/RPM	Manure
Jan	45,6	47,59853	7,931525	32,5	1	0,23	0,025	0,67	0,008438
Feb	34,2	63,18021	9,654705	32,5	1	0,23	0,03	0,67	0,008438
Mar	20,8	100,2235	12,59824	32,5	1	0,23	0,05	0,67	0,008438
Apr	7,1	141,2985	16,24455	32,5	0.6	0,23	0,05	0,67	0,008438
May	1,9	196,3626	20,911	32,5	0,6	0,23	0,05	0,67	0,008438
Jun	0,0	212,2946	23,40333	32,5	0,6	0,23	0,05	0,67	0,008438
Jul	0,0	231,4125	25,38035	32,5	0,6	0,23	0,02	0,67	0,008438
Aug	0,0	207,5142	25,36378	32,5	0.6	0,23	0,02	0,67	0,008438
Sep	0,5	152,6417	23,73377	32,5	0.6	0,23	0,02	0,67	0,008438
Okt	3,5	113,8375	19,83435	32,5	1	0,23	0,025	0,67	0,008438
Noc	12,1	81,14883	14,46483	32,5	1	0,23	0,025	0,67	0,008438
Dec	27,5	54,64711	9,425968	32,5	1	0,23	0,025	0,67	0,008438